Theoretical and Applied Fracture Mechanics 2 (1984) 259–286
North-Holland

STABLE GROWTH OF FRACTURE IN BRITTLE AGGREGATE MATERIALS

Michael P. WNUK *
Department of Civil Engineering, University of Wisconsin, Milwaukee, WI, USA

Zdeněk P. BAŽANT
Center for Concrete and Geomaterials, Northwestern University, Evanston, IL 60201, USA

Edward LAW
Northwestern University, Evanston, IL 60201, USA

Fracture of concrete is analyzed by combining the resistance curve (*R*-curve) approach with linearly elastic solutions for the energy release rate resulting from the quasi-static crack model of Wnuk, analogous to the D-BCS model of a stationary crack used in describing quasi-brittle fracture in metals. The *R*-curve, representing the crack length dependence of the energy consumed per unit fracture extension, is calculated using the concept of the energy separation rate associated with a finite crack growth steps. To simplify calculations, the tensile stress transmitted across the nonlinear zone ahead of the fracture front is assumed to be uniformly distributed over the entire nonlinear zone, even though in reality it must be a gradually declining stress resulting in strain-softening; and an infinite elastic medium loaded at infinity is assumed. These assumptions permit an easy solution with the help of Green's function for an infinite elastic medium. Application to bodies of finite size then requires assuming the nonlinear zone (fracture process zone) to be negligible with regard to specimen dimensions, crack length and ligament length. Even though this assumption is not always realistic, the end results, which are of practical importance, appear reasonable. The analysis leads to a nonlinear first-order ordinary differential equation for the *R*-curve, which is integrated numerically. The *R*-curves calculated in this manner can be closely fitted to data from previous fracture tests. Only two parameters, characterizing the initial and the final lengths of the nonlinear zone, need to be adjusted to test data.

Introduction

Inelastic behavior of brittle aggregate materials, such as concretes, mortars and rocks, arises not only from plastic slip but also and mainly, from internal fracturing (cracking) which causes a gradual degradation of material stiffness. Heterogeneity of geomaterials and their softening, which results from an accumulation of micro-defects dispersed randomly within the volume of a highly stressed material, are the primary reasons that impede direct applications of linear elastic fracture mechanics (LEFM) or elastic plastic fracture mechanics (EPFM) to concrete. Recently, successful representation of fracture test data and strength data have been obtained with finite element models in which the fracture process zone at the fracture front is considered to be finite and a suitable law for gradual reduction of the principal tensile stress ahead of the fracture front is introduced; see Hillerborg, Modéer and Petersson [1], Petersson [2] and Bažant and Oh [28,29], and Bažant [37]. Fracture predictions with these models require, however, the use of a finite element code which might be unnecessarily cumbersome for various simple situations. It is, therefore, of interest to develop approximate analytical solutions based on some simplifying assumptions. To make this possible, the problem must be simplified so that linear fracture mechanics could be applied for various simple specimen geometries in an approximate (equivalent) sense, in a similar manner as it has been done in ductile fracture mechanics. An approach of this kind is the objective of the present work.

We will analyze the so-called resistance curve (*R*-curve), which describes dependence of the energy

* Formerly visiting Professor at the Northwestern University.

consumed per unit fracture extension (or of fracture toughness) on the crack length, and, for the sake of simplicity, we will restrict this analysis to an infinitely extending linearly elastic continuum loaded at infinity, for which a simple Green's function exists. Application of our results to bodies of finite size and loads that are not infinitely remote is then possible by introducing the simplifying assumption that the R-curve remains the same. This assumption, which was proposed for metals by Krafft et al. [3,37], would be exact only if the fracture process zone at the fracture front was negligibly small as compared to body dimensions and the uncracked ligament length. However, experience with metals suggests that reasonable approximations are obtained even if the fracture process zone is finite.

In the present work, the propagation of fracture is envisioned as a sequence of finite growth steps or 'jumps', each of which is preceded by a build-up of microcracks and voids within a narrow damage band or crack band. The length and width of such a damage band is assumed to be small in comparison to the total crack or notch length and the specimen dimensions. Our model of quasi-static stable fracture employs the concept of 'energy separation rate', $\mathscr{G}^{\Delta}$, associated with a finite crack length increment, as opposed to the 'energy release rate', $\mathscr{G}_R$, used in the LEFM, which is applicable to a crack extending in a continuous manner. While the latter quantity measures the apparent fracture toughness represented by the so-called resistance curve, the former quantity appears to be a more realistic measure of the true material toughness. This quantity is invariant with regard to the amount of stable cracking which precedes unstable catastrophic fracture.

Previous work

Occurrence of slow stable crack growth in the early stage of fracture in mortar or concrete is a widely recognized phenomenon. Due to their aggregate structure and their ability to undergo progressive microcracking, these materials do not follow the linear fracture mechanics laws unless the size of the specimen and the length of the uncracked ligament is substantially larger than the size of the characteristic nonlinear zone (dictated by size of aggregate, fibers or inclusions). In consequence, fracture toughness is not a unique material property, as required by the LEFM, but it depends on the specimen size and on the length of crack extension. Since in mortars and concretes the typical size of aggregate, or the typical length of fibers in a fiber reinforced concrete, is on the order of one inch, usual size laboratory tests do not yield a unique, size-independent, fracture parameter.

An approach which is capable of taking the nonlinear effects of such nature into account, and which has been already developed for metals [4] and geomaterials (Hoagland et al. [6]; Schmidt and Lutz, [7]; Wnuk and Mura, [8], Wecharatana and Shah, [27]), consists in using a variable fracture toughness depending on crack extension length. This is described in terms of the crack resistance curve, called the R-curve. An R-curve is obtained by plotting a certain parameter characterizing an energy absorbed during the fracture process at each step of crack growth as a function of the crack length. Since we model fracture that occurs at a continuously increasing load, the classical formula for the energy release rate at a constant load, namely $\mathscr{G}_I = (P^2/2t_n)\mathrm{d}Z/\mathrm{d}a$, does not apply; here P is the load, Z is the compliance, which is a function of the current crack length a, and t_n is the thickness in the plane of crack. To remedy this drawback, certain new approaches have been suggested, one of which provides a direct extension of this formula through an introduction of so-called 'modified' strain energy release rate (Wecharatana and Shah, [27]). To apply this modified approach, however, the rate of change (per unit crack extension) of the reloading compliance, $\mathrm{d}\mathscr{G}_R/\mathrm{d}a$, and the permanent deformation upon unloading (δ_{irrev}), have to be either calculated or measured, which is not an easy task.

An alternative approach, proposed for metals and rocks (Wnuk, [33], Wnuk and Mura, [8]) is based on the so-called 'final stretch' concept, which in turn may be derived from the concept of true fracture energy or 'essential work of fracture'. Physical assumptions of similar nature underlay the models proposed by Broberg [10], Cotterell [9], Miller and Kfouri [11] and Kfouri and Rice [12]. The energy separation rate, which represents the energy absorbed within the process zone during a fracture increment, is invariant with regard to stable crack extension and, therefore, it represents a true fracture parameter.

Fracture criterion and the equation of motion of a quasi-static crack

Consider the small zone of material immediately adjacent to the crack front, called the fracture process zone or end zone. It may be assumed that within this zone the laws of the classical fracture mechanics break down, and that instead of $r^{-1/2}$ stress singularity one has a certain unknown distribution of the restraining force, say $S(x_1)$, defined within the interval $0 \le x_1 \le R$, where x_1 is the distance from the crack tip and R is the extent of the nonlinear zone (Fig. 1). On the basis of the Green function for an infinite half space, the stress intensity factor may be expressed as

$$K_1 = 2\sqrt{\frac{a}{\pi}} \int_0^a \frac{p(x)\,dx}{\sqrt{a^2 - x^2}} \tag{1}$$

in which $p(x)$ is an even function which represents the stress acting on the crack surface. The 'toughness' associated with a quasi-static crack, K_R, is interpreted as the stress intensity factor arising from application of the restraining stress $S = S(x)$ transmitted through a fictitious crack extending up to $x = a + R$ ($a \le |x| \le a + R$), as shown in Fig. 1. If we replace a by $(a + R)$ and set

$$p(x) = \begin{cases} 0 & \text{for } 0 \le x \le a \\ S(x) & \text{for } a < x \le a + R \end{cases} \tag{2}$$

then integral (1) becomes

$$K_R = \left[2\sqrt{\frac{a+R}{\pi}} \int_a^{a+R} \frac{S(x)\,dx}{\sqrt{(a+R)^2 - x^2}} \right]_{R \ll a} = 2\sqrt{\frac{a+R}{\pi}} \frac{1}{\sqrt{2(a+R)}} \int_a^{a+R} \frac{S(x)\,dx}{\sqrt{a+R-x}}. \tag{3}$$

When we substitute x_1 for $x - a$, Eq. (3) reduces to

$$K_R = \sqrt{\frac{2}{\pi}} \int_0^R \frac{S(x_1)\,dx_1}{\sqrt{R - x_1}}. \tag{4}$$

For a growing crack the quantities R and S are dependent on the current crack length, i.e.

$$R = R(a), \qquad S = S(x_1, a). \tag{5}$$

Therefore, the integral represented by Eq. 4 and used as a measure of material toughness, is also crack length dependent, i.e. $K_R = K_R(a)$. This observation suggests that the quantity K_R may be used merely to

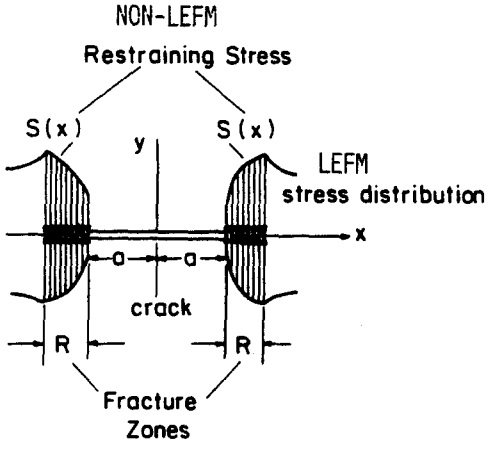

Fig. 1. Fictitious crack model.

measure an *apparent* toughness which is not invariant with regard to the crack extension occurring prior to the unstable fracture. For the same reason, the energy release rate, as defined in the realm of the linear elastic fracture mechanics, i.e.

$$\mathcal{G}_R = \frac{2}{\pi E_1}\left(\int_0^R \frac{S(x_1)\,dx_1}{\sqrt{R-x_1}}\right)^2, \quad \text{with } E_1 = \begin{cases} E & \text{for plane stress} \\ (1-\nu^2)^{-1}E & \text{for plane strain} \end{cases} \tag{6}$$

also becomes a variable which varies with crack extension. Within the socalled 'small-scale yielding' range, that is, when the extent of the end zone is much smaller than the crack half-length ($R \ll a$) and much smaller than the specimen size, the use of the fracture parameters $\mathcal{G}_R$, K_R or R is optional and equivalent, since all three quantities are uniquely related once a certain distribution of the stresses over the end zone is specified. For instance, if we assume a constant value oft he restraining stress $S(x_1) = \sigma_0$ (see Fig. 2a), then integral (4) yields

$$K_R = \sqrt{\frac{2}{\pi}}\,\sigma_0 \int_0^R \frac{dx_1}{\sqrt{R-x_1}} = \sqrt{\frac{2}{\pi}}\,\sigma_0 2\sqrt{R} \tag{7}$$

or

$$R = \frac{\pi}{8}(K_R/\sigma_0)^2. \tag{8}$$

If, on the other hand, the restraining stress is allowed to vary in a bilinear fashion, first increasing from zero to a maximum value σ_0 attained at a distance β from the crack front and then maintained at a constant level σ_0 for $\beta \le x_1 \le R$, as shown in Fig. 2b, then integral (4) leads to

$$R = \frac{\pi}{8}\left(\frac{K_R}{\sigma_0}\right)^2 \frac{\frac{9}{4}(\beta/R)^2}{\left[1-(1-\beta/R)^{3/2}\right]^2}, \tag{9}$$

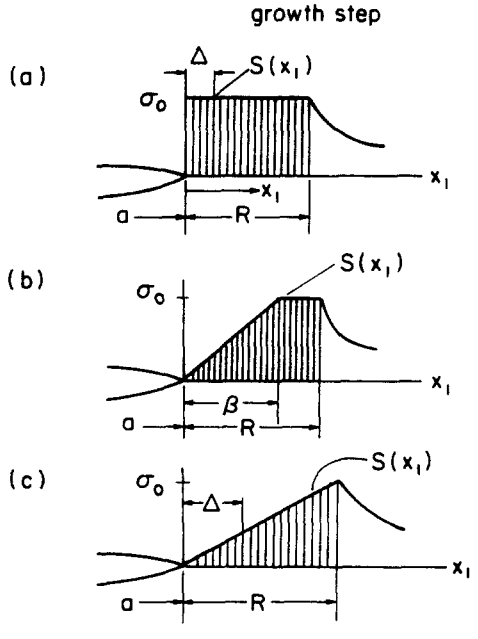

Fig. 2. Three types of cohesive (restraining) stress distribution considered in the text.

where β and σ_0 are two additional constants. For a linear distribution of the restraining stress over the entire end zone (see Fig. 2c), Eq. 9 yields

$$R|_{\beta\to R}=\frac{\pi}{8}\frac{9}{4}\left(\frac{K_R}{\sigma_0}\right)^2. \tag{10}$$

The formulae (9) and (10) result by substituting the bilinear distribution

$$S(x_1)=\begin{cases}(\sigma_0/\beta)x_1, & 0\le x_1\le\beta\\ \sigma_0, & \beta\le x_1\le R\end{cases} \tag{11}$$

into Eq. 4 and carrying out the integration, i.e.

$$K_R=\sqrt{\frac{2}{\pi}}\left\{\int_0^\beta\frac{(\sigma_0/\beta)x_1\,dx_1}{\sqrt{R-x_1}}+\sigma_0\int_\beta^R\frac{dx_1}{\sqrt{R-x_1}}\right\}. \tag{12}$$

Equations (8) and (9) are examples of the so-called finiteness condition, i.e. conditions for the stress $S(x_1)$ in the nonlinear zone to remain finite. For a general case of an arbitrary distribution of stress $S(x_1)$, this condition is given by Eq. 4.

To derive the governing equation of motion for a quasi-static crack which interacts with the damage band formed ahead of the front, one needs to solve a boundary value problem for which the traction $p(x)$ is prescribed over the crack surface, as in Eq. 2, while the displacement component normal to the crack plane u_y is set zero along the symmetry line ($y=0$) beyond the end zone, i.e. for $|x|>a+R$, or $x_1>R$. For the three idealized distributions of stress $S(x_1)$ considered here, the solutions which define the displacement u_y within the end zones ($0\le x_1\le R$) are as follows:

(a) Constant restraining stress (Fig. 2a):

$$u_y(x_1,R)=\frac{4\sigma_0}{\pi E_1}R\left\{\sqrt{1-\frac{x_1}{R}}-\frac{x_1}{2R}\log\frac{1+\sqrt{1-(x_1/R)}}{1-\sqrt{1-(x_1/R)}}\right\}. \tag{13}$$

(b) Bilinear restraining stress (Fig. 2b):

$$u_y(x_1,\beta,R)=\left(\frac{4\sigma_0}{\pi E_1}\right)Rg(\beta/R)F(x_1,\beta,R), \tag{14}$$

in which

$$g(\beta/R)=\frac{4}{3}\left[1+\frac{1-\beta/R}{1+\sqrt{1-\beta/R}}\right],$$

$$F(x_1,\beta,R)=B+\tfrac{1}{2}A\left[\frac{\beta-x_1}{2R}\log\left|\frac{B+B_0}{B-B_0}\right|-B_0B\right]+\frac{AR}{4\beta}\left[\frac{\beta^2-x_1^2}{2R^2}\log\left|\frac{B-B_0}{B+B_0}\right|\right.$$
$$\left.-\frac{x_1^2}{2R^2}\log\left|\frac{B+1}{B-1}\right|-(1-B_0)\left(1+\frac{x_1}{R}\right)B+\tfrac{1}{3}(1-B_0^3)B\right],$$

$$A=\frac{3\beta}{2R}\left[1-\left(1-\frac{\beta}{R}\right)^{3/2}\right]^{-1},\qquad B_0=\sqrt{1-\frac{\beta}{R}},\qquad B=\sqrt{1-\frac{x_1}{R}}.$$

(c) Linear restraining stress (Fig. 2c):

$$u_y(x_1, R) = \left(\frac{4\sigma_0}{\pi E_1}\right) R \left\{ \left(1 - \frac{x_1}{2R}\right)\sqrt{1 - \frac{x_1}{R}} + \frac{1}{4}\left(\frac{x_1}{R}\right)^2 \log \frac{1 - \sqrt{1 - (x_1/R)}}{1 + \sqrt{1 - (x_1/R)}} \right\}. \tag{15}$$

Derivation of the last formula is given in Appendix A, while Eqs. 13 and 14 were derived by Rice [13] and Knauss [32], respectively.

In contrast to the energy release rate $\mathcal{G}_R$ defined in accordance with the fundamental concepts of LEFM (see Eq. 6), we will employ a somewhat different measure of material toughness for the early stages of fracture formed by coalescence of micro-cracks. We imagine a discontinuous crack extension consisting of a sequence of *finite* growth steps, each of equal length Δ. We now need to modify the well-known integral representing the energy release rate

$$\mathcal{G} = \lim_{\delta a \to 0} \left\{ \frac{2}{\delta a} \int_a^{a+\delta a} S(x) \delta u_y(x, a)\, dx \right\} \tag{16}$$

to introduce a finite growth step, Δ. This may be done as follows:

$$\mathcal{G}^{\Delta} = \lim_{\delta a \to \Delta} \left\{ \frac{2}{\delta a} \int_a^{a+\delta a} S(x) \delta u_y(x, a, \Delta)\, dx \right\}. \tag{17}$$

This is called the energy separation rate, which may be interpreted as the work done to produce crack extension Δ. The associated increment in the crack opening is $\delta u_y = u_y(x, a + \delta a, \Delta) - u_y(x, a, \Delta)$.

Using the expression given by Eq. 17 as a measure of the intensity of the stress field induced in the immediate vicinity of the crack tip, we postulate that fracture will occur whenever the fracture work (or energy separation rate) attains a certain critical value, $\hat{\mathcal{G}}$:

$$\lim_{\delta a \to \Delta} \left\{ \frac{2}{\delta a} \int_a^{a+\delta a} S(x) \delta u_y(x, a, \Delta)\, dx \right\} = \hat{\mathcal{G}}. \tag{18}$$

The quantity $\hat{\mathcal{G}}$ represents a material constant, sometimes called the essential work of fracture (Cotterell [9]), and it in turn may be related to other fundamental properties of material (Wnuk and Mura [34]). Integral (17) is difficult to evaluate, at least for the case of an arbitrary distribution of the restraining stress $S(x)$. However, it may be shown (see Appendix B) that for the three particular cases of a constant, a linear and a bilinear distribution of S, the evaluation of the left-hand side of our fracture criterion (Eq. 18) may be greatly simplified. Simplifications of this kind lead to the so-called 'final stretch" criterion of fracture (Wnuk [8,33]). As may be shown, the choice of a particular shape of the S-function has little effect on the predictions regarding the shape of the R-curve (the final product of the analysis); see Fig. 3. Therefore, we will restrict our further consideration to the most simple choice of the S-function, i.e., $S(x_1) = \sigma_0$ for

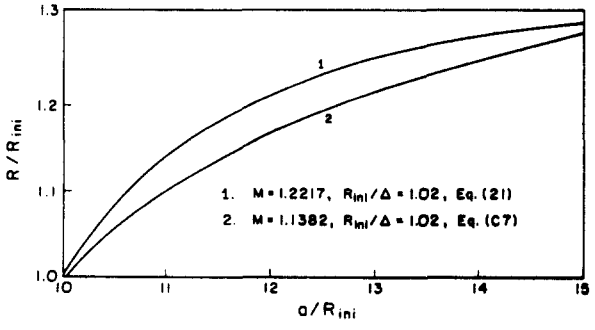

Fig. 3. R-curves obtained for constant (case a) and linear (case c) restraining stress distributions.

$0 < x_1 \leq R$. As shown in Appendix C, we have in this case

$$\frac{8\sigma_0^2}{\pi E_1}\left\{\Delta\frac{dR}{da}+\frac{R}{\Delta}-\sqrt{\frac{R}{\Delta}\left(\frac{R}{\Delta}-1\right)}-\tfrac{1}{2}\log\frac{\sqrt{R/\Delta}-\sqrt{R/\Delta-1}}{\sqrt{R/\Delta}+\sqrt{R/\Delta-1}}\right\}=\hat{\mathcal{G}}. \tag{19}$$

Furthermore, introducing the quantity

$$M=\frac{\pi}{8}\frac{\hat{\mathcal{G}}E_1}{\sigma_0^2\Delta} \quad \text{or} \quad M=\frac{\pi}{8}\left(\frac{E_1}{\sigma_0}\right)\left(\frac{\hat{\delta}}{\Delta}\right) \tag{20}$$

called the tearing modulus, the equation defining an R-curve, $R = R(a)$, reads

$$\frac{dR}{da}=M-\frac{R}{\Delta}+\sqrt{\frac{R}{\Delta}\left(\frac{R}{\Delta}-1\right)}+\tfrac{1}{2}\log\frac{\sqrt{R/\Delta}-\sqrt{R/\Delta-1}}{\sqrt{R/\Delta}+\sqrt{R/\Delta-1}}. \tag{21}$$

This is a nonlinear first-order differential equation for which the initial condition $R = R_{ini}$ at $a = a_0$ has to be provided. Then the integration can be carried out numerically (see the next section for comparison with experimental data). The outcome is an R-curve valid for the case when the size of the end zone is much smaller than the length of the crack. Note, however, that no restrictions have been imposed on the size of the growth step (Δ) versus the extent of the nonlinear zone (R).

Finally, the dependence of load on the crack extension may be predicted by specifying the stress intensity factor as a function of the specimen shape parameters θ_i, type of loading and the crack length, i.e.,

$$K=\sigma\sqrt{a}\,\phi(\theta_i, a). \tag{22}$$

If the applied stress σ is characterized by the non-dimensional loading parameter

$$Q=\frac{\pi\sigma}{2\sigma_0} \tag{23}$$

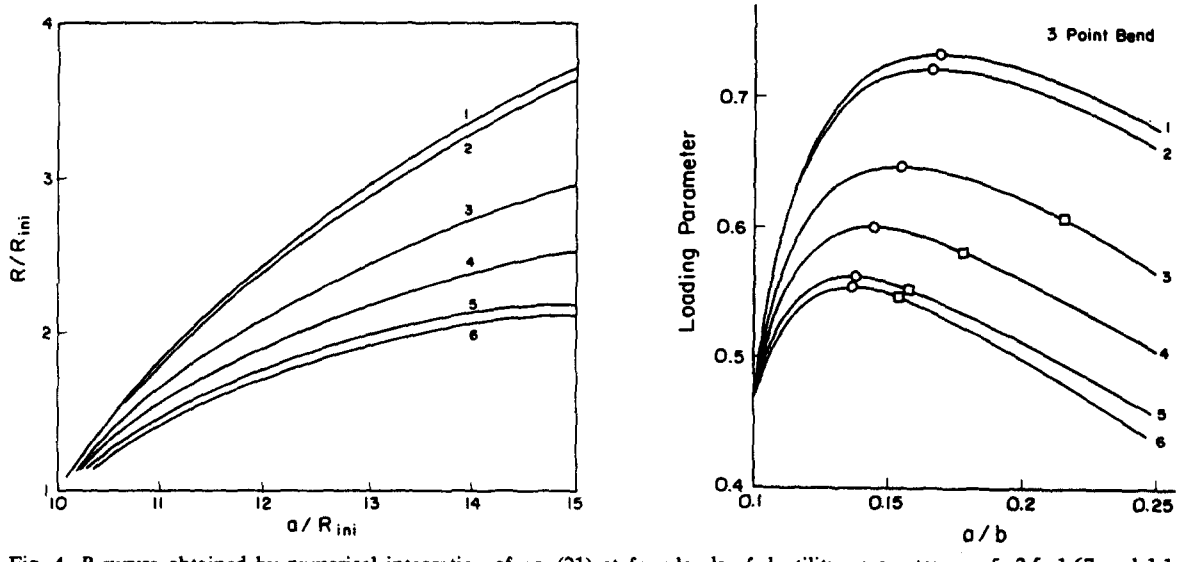

Fig. 4. R-curves obtained by numerical integration of eq. (21) at four levels of ductility parameter $\rho_i = 5$, 2.5, 1.67 and 1.1. The upper-most and lower-most curves resulted from the asymptotic equations valid in the limit of $\Delta \ll R$ (curve 1) and $\Delta \gg R$ (curve 6, Eq. C8).

Fig. 5. Nondimensional loading parameter Q shown as a function of extension of a stable crack, Δa, recorded in a 3-point bend specimen for the 4 levels of ductility parameter used in Fig. 4. Circles mark the terminal instabilities attained in a load-controlled test, while the stars denote the instabilities reached in a displacement-controlled test.

then one obtains a simple relation between an R-curve and a Q-curve (load vs. increment of crack extension), namely

$$Q(a) = \phi^{-1}\sqrt{\frac{2\pi R(a)}{a}}\,. \tag{24}$$

Examples of integration of the governing equation (21) are given in Fig. 4, while the Q-curves for three-point bend specimens are shown in Fig. 5. We note that both sets of curves are strongly affected by the assumed value of the ratio

$$\rho_i = R_{\text{ini}}/\Delta. \tag{25}$$

As it turns out, the size of the growth step (Δ) when compared against the initial extent of the nonlinear zone, R_{ini}, provides an excellent measure of material ductility or brittleness. From Figs. 4 and 5 we conclude that the two opposite limits of material behavior are obtained as follows:

$$\begin{aligned} &\Delta \ll R, \quad \text{ductile behavior,} \\ &\Delta \simeq R, \quad \text{brittle behavior.} \end{aligned} \tag{26}$$

Comparisons of the experimental and theoretical results

Most of the data available in the literature [14–27] are given in terms of the apparent fracture toughness (R-curves) and the curves of maximum load vs. the critical crack length.

To fit these data, we will have to define the optimum choice of fracture parameters that enter our model. We note that there are two undetermined parameters in Eq. 21, namely: (i) tearing modulus, M, and (ii) near-tip stress distribution parameter, which may be called ductility index, R_{ini}/Δ. To obtain the best fit values of these parameters, we have employed the Hermite-type interpolation, using the initial slope of an experimentally obtained R-curve and the coordinates of some point on such a curve located far from the initiation point to obtain two equations for two unknown quantities, M and R_{ini}/Δ. If the initial slope $\gamma = (\mathrm{d}R/\mathrm{d}a)_{\text{ini}}$, and the final plateau R_{ss} of the R-curve, are known, then application of the Hermite interpolation combined with the differential equation defining an R-curve leads to the following equations for M and R_{ini}/Δ:

$$\begin{aligned} &M - \rho_i + \sqrt{\rho_i(\rho_i - 1)} + \tfrac{1}{2}\log\frac{\sqrt{\rho_i} - \sqrt{\rho_i - 1}}{\sqrt{\rho_i} + \sqrt{\rho_i - 1}} = \gamma, \\ &M - \rho_{\text{ss}} + \sqrt{\rho_{\text{ss}}(\rho_{\text{ss}} - 1)} + \tfrac{1}{2}\log\frac{\sqrt{\rho_{\text{ss}}} - \sqrt{\rho_{\text{ss}} - 1}}{\sqrt{\rho_{\text{ss}}} + \sqrt{\rho_{\text{ss}} - 1}} = 0. \end{aligned} \tag{27}$$

Eliminating the tearing modulus M and denoting the ratio $R_{\text{ss}}/R_{\text{ini}}$ by m, we reduce this system to a single equation

$$\begin{aligned} &\gamma - m\rho_i + \sqrt{m\rho_i(m\rho_i - 1)} + \tfrac{1}{2}\log\frac{\sqrt{m\rho_i} - \sqrt{m\rho_i - 1}}{\sqrt{m\rho_i} + \sqrt{m\rho_i - 1}} + \rho_i - \sqrt{\rho_i(\rho_i - 1)} \\ &\quad - \tfrac{1}{2}\log\frac{\sqrt{\rho_i} - \sqrt{\rho_i - 1}}{\sqrt{\rho_i} + \sqrt{\rho_i - 1}} = 0 \end{aligned} \tag{28}$$

which is of the form

$$F(\gamma, m, \rho_i) = 0. \tag{29}$$

Since both initial slope and the upper plateau, i.e., γ and m, may be read from the experimentally determined R-curves, the only unknown is ρ_i. It may be found numerically for a certain range of the constants γ and m. This procedure was applied whenever possible in choosing the optimum values of the tearing modulus and the near-tip stress distribution parameter R_{ini}/Δ.

The location of the maximum load point was determined from the equation

$$\frac{dR}{da} = \left[\frac{\partial R_A}{\partial a}\right]_Q \tag{30}$$

in which the symbol R_A denotes intensity of the applied stress field relative to loading parameter Q and the K-factor as follows:

$$R_A = \frac{\pi}{8}\left(\frac{K_I}{\sigma_0}\right)^2 = \frac{a}{2\pi}Q^2\phi^2, \quad \phi = K_I/\sigma\sqrt{a}, \quad Q = \pi\sigma/2\sigma_0. \tag{31}$$

Specific relations of this type, corresponding to various geometrical configurations frequently used in fracture tests, are given in Appendix D.

Let us now discuss a typical fitting problem using the three R-curves obtained recently in Wecharatana and Shah's experiments. Using their data for three materials of low strength: (a) concrete (C) ($E = 3 \times 10^6$ psi, $\sigma_0 = 700$ psi), (b) mortar, Mix 1 (M1), $E = 2.5 \times 10^6$ psi, effective stress $\sigma_0 = 620$ psi, and (c) mortar, Mix 2 (M2), $E = 2.2 \times 10^6$ psi, effective stress $\sigma_0 = 590$ psi (see their Fig. 12 and the corresponding regression equations listed in their Table 4 pertaining to the R-curve data), the experimental R-curves may be reduced to two normalized R-curves, since the R-curves for concrete (C) and mortar Mix 2 (M2), when plotted in terms of nondimensional variables $\mathcal{G}/\mathcal{G}_{ini}$ and a/R_{ini}, converge to just one curve. To fulfill the requirement of smallness of the R/a ratio, the current crack length of 5 inches is considered as the initial crack size, and then the following data may be read from the R-curves shown in Fig. 12 by Wecharatana and Shah [27]:

$$\mathcal{G}_{ini} = [\mathcal{G}_R]_{a=5''} = \begin{cases} 0.718 \text{ lb./in.} & \text{for C} \\ 0.526 \text{ lb./in.} & \text{for M2} \\ 0.465 \text{ lb./in.} & \text{for M1} \end{cases}. \tag{32}$$

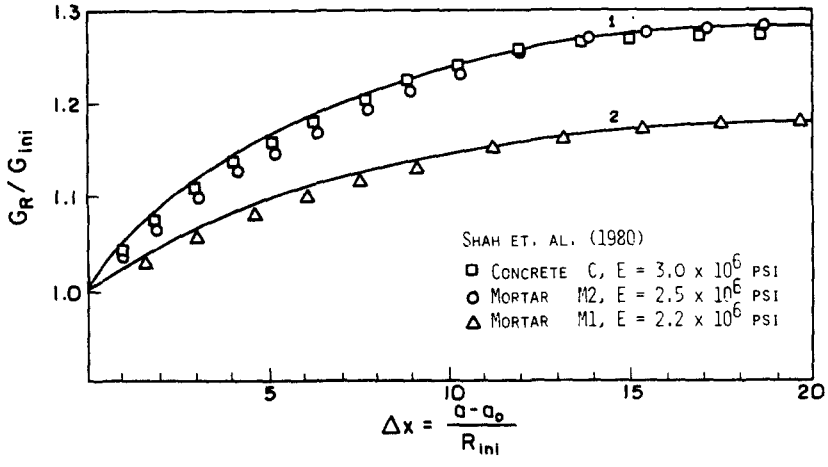

Fig. 6. Comparison between the test data, Ref. [27], and the predictions of the present model. Curves 1 and 2 were determined by Eqs. (40) and (C8a).

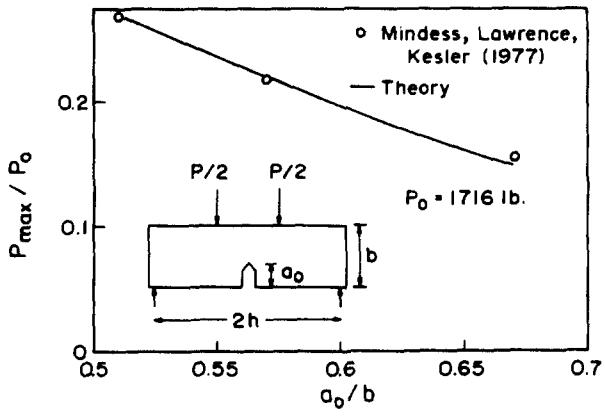
o Mindess, Lawrence, Kesler (1977)
— Theory
P/2 P/2
P_0 = 1716 lb.
b
a_0
2h
P_{max}/P_0
a_0/b

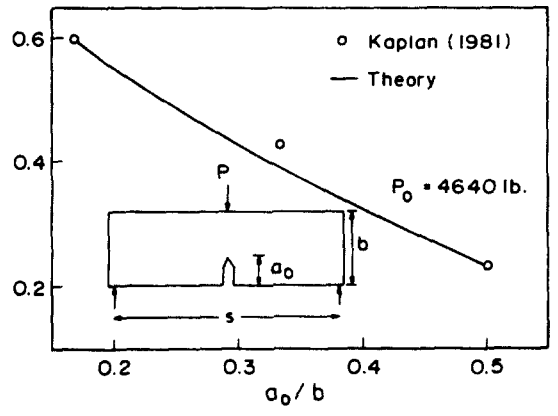
o Kaplan (1981)
— Theory
P
P_0 = 4640 lb.
b
a_0
s
a_0/b

(7a)

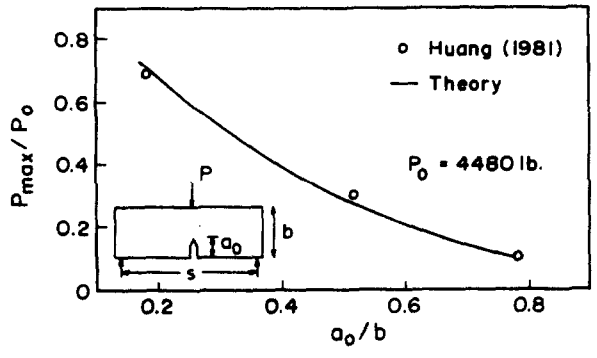
o Huang (1981)
— Theory
P
P_0 = 4480 lb.
b
a_0
s
P_{max}/P_0
a_0/b

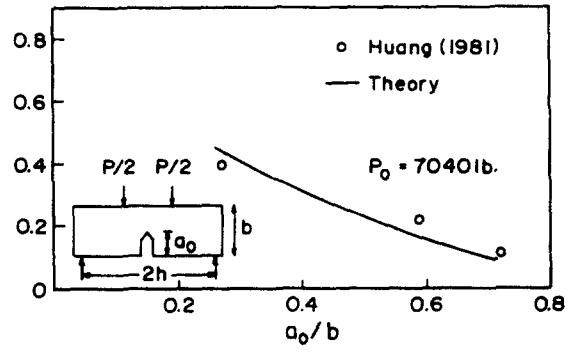
o Huang (1981)
— Theory
P/2 P/2
P_0 = 7040 lb.
b
a_0
2h
a_0/b

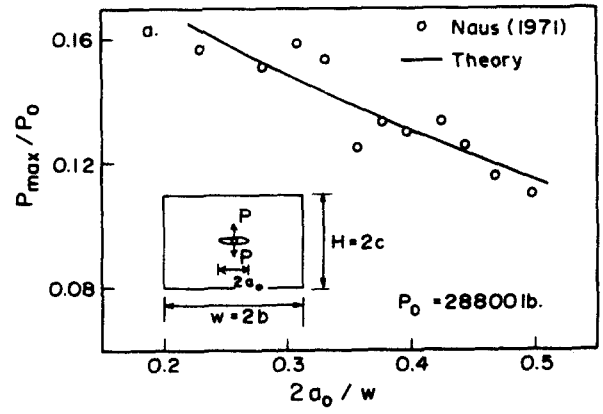
a.
o Naus (1971)
— Theory
P
H=2c
w=2b
P_0 = 28800 lb.
P_{max}/P_0
$2a_0/w$

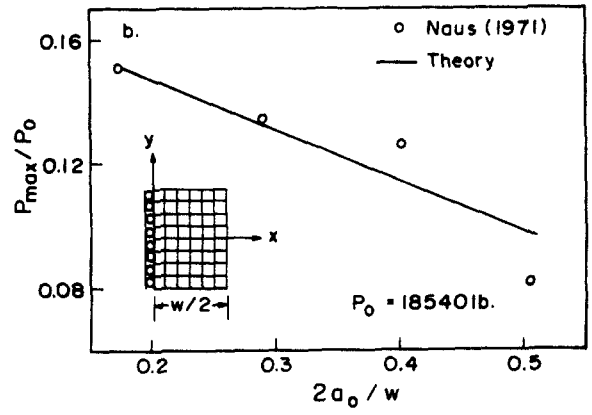
b.
o Naus (1971)
— Theory
y
x
w/2
P_0 = 18540 lb.
P_{max}/P_0
$2a_0/w$

(7b)

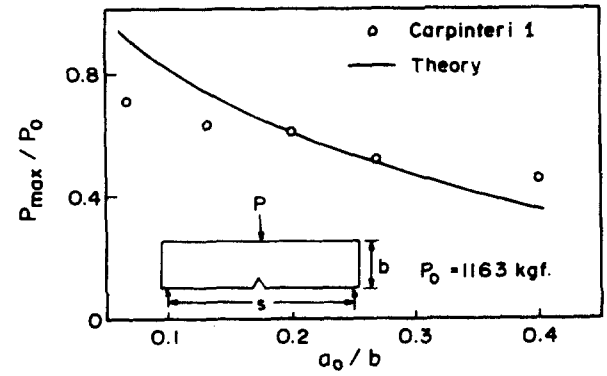
o Carpinteri 1
— Theory
P
b
s
P_0 = 1163 kgf.
P_{max}/P_0
a_0/b

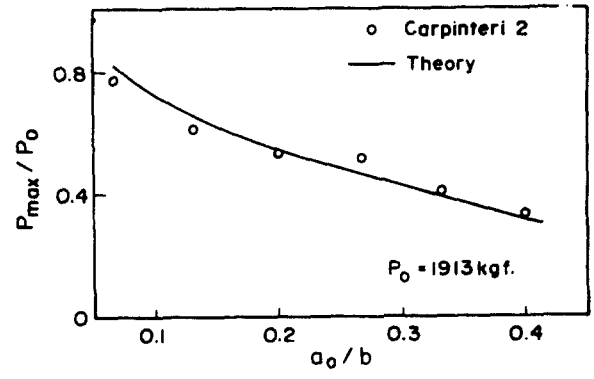
o Carpinteri 2
— Theory
P_0 = 1913 kgf.
P_{max}/P_0
a_0/b

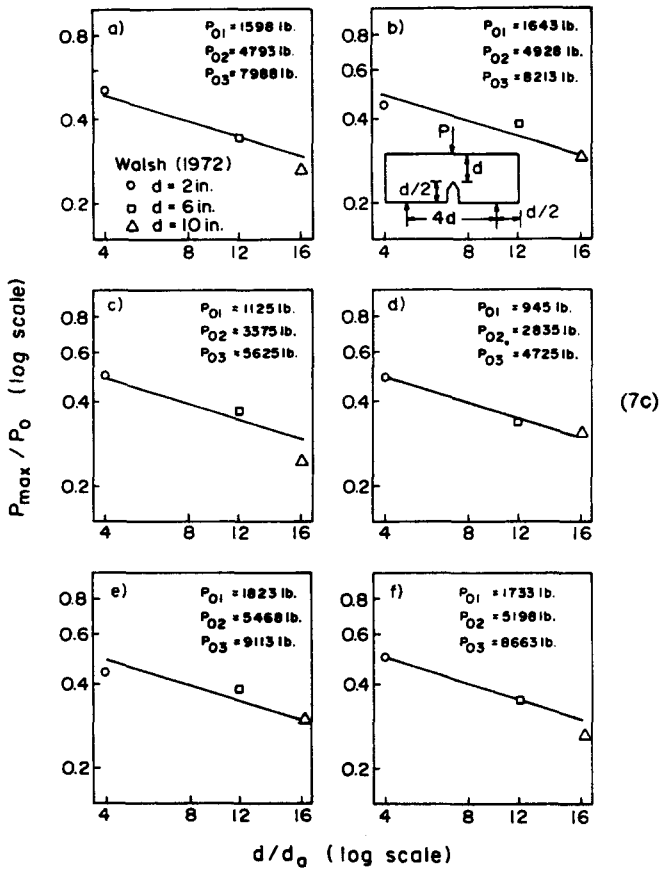

(7c)

Fig. 7. Maximum load fracture test data (data points and the source are indicated in each box) compared with the theoretical predictions of the present model.

The 'steady-state' values of the apparent material toughness, as given by the same authors, are

$$\mathcal{G}_{ss} = [\mathcal{G}_R]_{a=20''} = \begin{cases} 0.920 \text{ lb./in.} & \text{for C} \\ 0.670 \text{ lb./in.} & \text{for M2} \\ 0.558 \text{ lb./in.} & \text{for M1} \end{cases} . \tag{33}$$

The size of the nonlinear zone, R_{ini}, measured at the current crack length of 5 inches, can be estimated from the equation

$$R_{ini} = (\pi/8)\left(nE\mathcal{G}_{ini}/\sigma_0^2\right) \tag{34}$$

in which the empirical factor n usually varies between 1 and 2.6, and the effective stress σ_0 is known. Based on this, the following estimates for the extent of the nonlinear zone may be obtained:

$$R_{ini} = \begin{cases} 1.00'' & \text{for C} \\ 0.78'' & \text{for M2} \\ 0.66'' & \text{for M1} \end{cases} . \tag{35}$$

The interval for the variation of coefficient n has been restricted to $1.7 < n < 1.74$. These numbers are then

employed to normalize the increment of stable cracking according to the formula

$$\Delta X = (a - a_0)/R_{\text{ini}} \tag{36}$$

in which a_0 is taken to correspond to the current crack length of 5 inches. Note that the ratio of the extent of the nonlinear zone to the current crack length lies within the range

$$(R/a)_{\text{ss}} \leq R/a \leq (R/a)_{\text{ini}} \tag{37}$$

and, for the materials under consideration, one obtains the estimates

$$(R/a)_{\text{ini}} = \begin{cases} 1/5 = 0.2 & \text{for C} \\ .78/5 = 0.156 & \text{for M2} \\ .66/5 = 0.132 & \text{for M1} \end{cases} \tag{38}$$

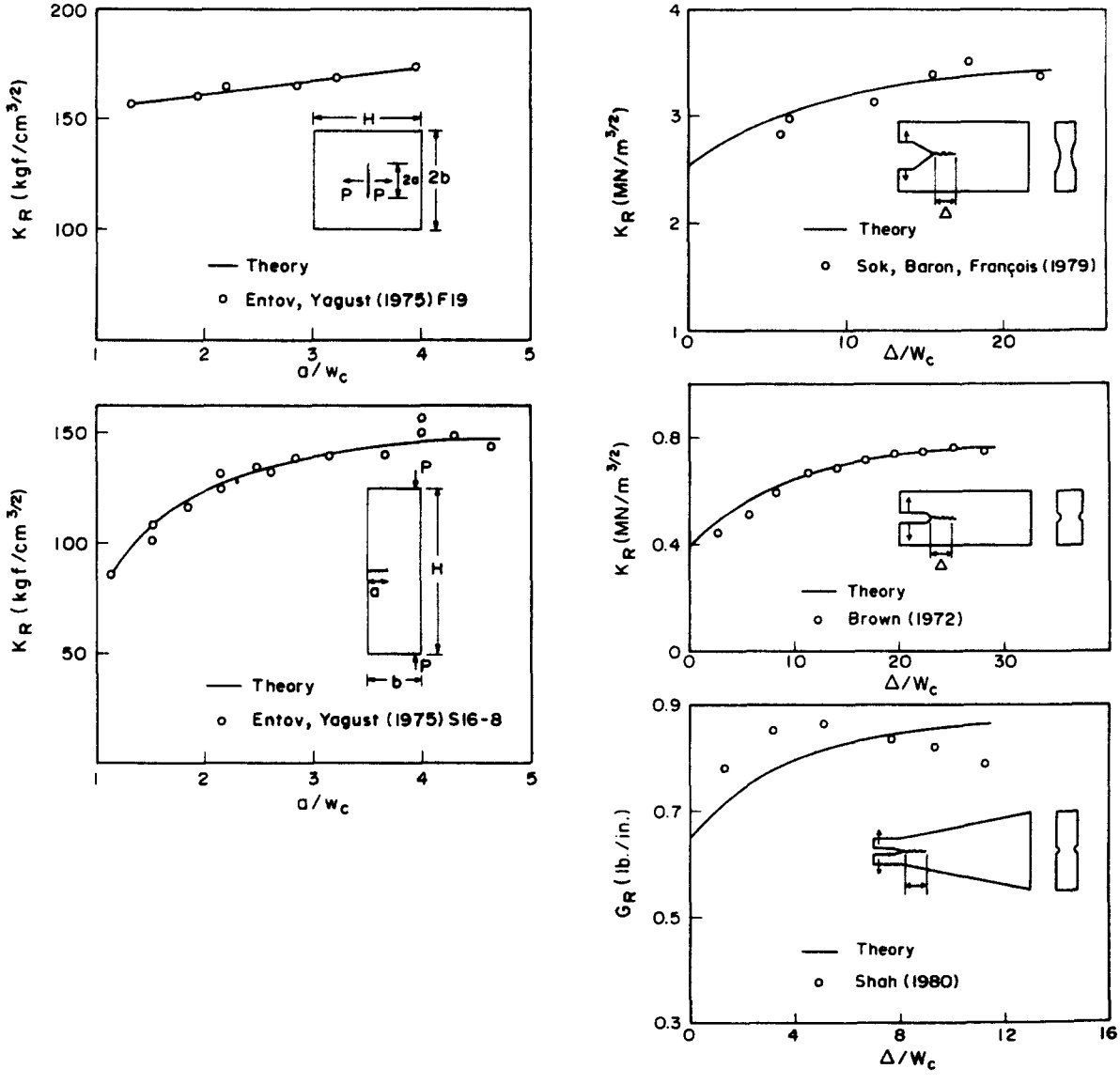

Fig. 8. *R*-curve fracture test data compared with the predictions (continuous curves) derived from the present model.

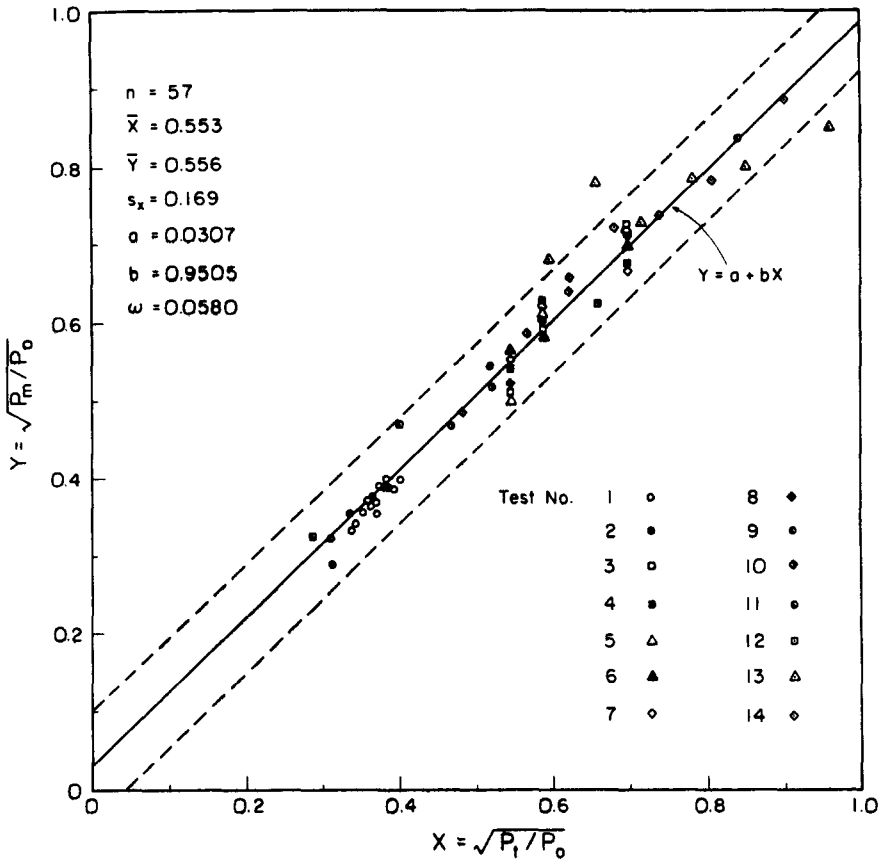

(a)

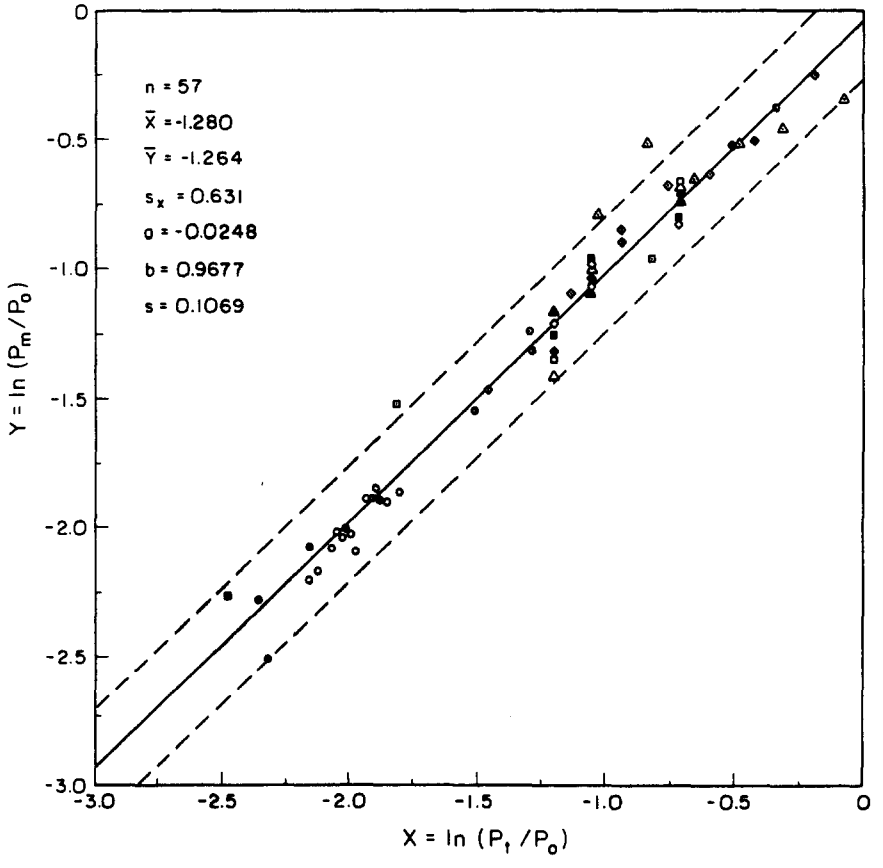

(b)

Fig. 9. Statistical scatter of the experimental data about the best fit regression line, $Y = a + bX$. The vertical scale represents (a) square root or (b) logarithm of the nondimensional maximum load.

and

$$(R/a)_{ss} = \begin{cases} 1.28/20 = 0.064 & \text{for } C \\ .99/20 = 0.050 & \text{for } M2\,. \\ .792/20 = 0.040 & \text{for } M1 \end{cases} \tag{39}$$

Such a range of R/a values suggests a relatively low level of material toughness (brittle limit of behavior), which justifies applicability of the asymptotic equation (C8a). Figure 6 compares the experimental curves with the theoretical curves obtained by numerical integration of Eq. (C8a) for the initial values:

$$\begin{aligned} &\text{curve 1: } (\mathrm{d}R/\mathrm{d}a)_{\mathrm{ini}} = 0.067, \qquad R_{\mathrm{ini}}/\Delta = 1.53, \\ &\text{curve 2: } (\mathrm{d}R/\mathrm{d}a)_{\mathrm{ini}} = 0.035, \qquad R_{\mathrm{ini}}/\Delta = 1.65 \end{aligned} \tag{40}$$

which were chosen so as to obtain the best fit.

Table 1 summarizes the results of similar analyses of other typical experimental data available in the literature, Figs. 7–8 illustrate the match between theoretical and experimental results. In addition, Figs. 9 and 10 shows the results of a statistical analysis of the deviations of theoretical values from the measured ones. As may be seen from Fig. 10a, the coefficient of variation for the deviations of R-curve predictions is roughly 7%, and that for the deviations of the maximum predictions does not exceed 5%, as seen from Fig. 10b.

The same degree of accuracy has recently been obtained with another nonlinear fracture model for concrete (Bažant and Oh, [28]), which requires finite element solution of the field problem. That model is, however, more general in various respects. It does not require the fracture process zone (end zone) to be negligibly small compared to the cross section and ligament dimensions, and it permits considering the effect of boundaries or loads that are close to the fracture process zone or intersect it. The effect of compressive normal stresses parallel to the crack plane can be considered in that model, in quite a natural way. Furthermore, the effects of reinforcement and bond slip, as well as nonlinear material behavior outside the fracture process zone, can be considered in that model.

In judging the meaning of the coefficients of variation for the deviations from test data, one should also note that, in contrast to the present theory, the values of the fracture parameters for various concretes were

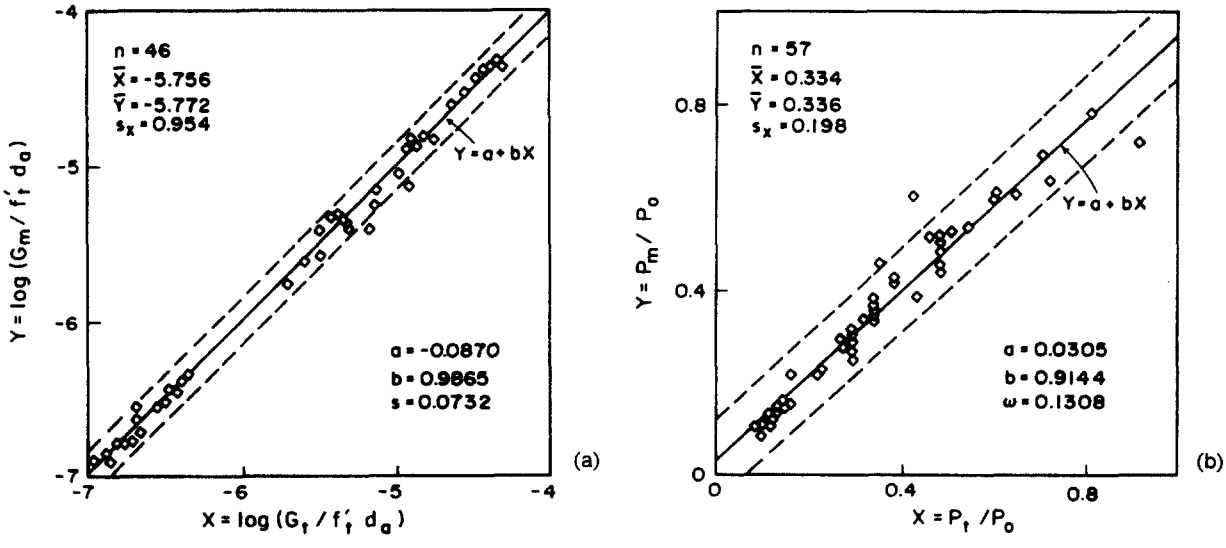

Fig. 10. Summary of statistical scatter of the fracture test data concerning (a) R-curve, and (b) maximum load obtained in various concretes in independent investigations.

Table 1
Coefficients obtained for various test data

Test series		σ_0 [psi]	$\mathcal{G}_{ini}$ [lb/in]	γ	n	ρ_i	R_{ini} [in]	M
Naus	1	800	0.1648	1.0	1.0	2.0	0.45	2.47
	2							
Walsh	1	680	0.1071	1.0	1.0	1.5	0.3	2.29
	2	750	0.1052	1.0	1.0	1.5	0.3	2.29
	3	480	0.0679	1.0	1.0	1.5	0.3	2.29
	4	430	0.0520	1.0	1.0	1.5	0.3	2.29
	5	840	0.1148	1.0	1.0	1.5	0.3	2.29
	6	750	0.1094	1.0	1.0	1.5	0.3	2.29
Mindess		870	0.0924	1.0	1.7	1.5	0.3	2.47
Kaplan		580	0.0613	1.0	1.0	2.0	0.3	2.47
Huang	1	660	0.2842	1.0	2.0	2.0	0.8	2.47
	2	660	0.1421	1.0	1.0	3.0	0.4	2.47
Carpinteri	1	441	0.1926	1.0	1.0	2.0	1.05	2.47
	2	726	0.3216	1.0	1.0	2.0	0.75	2.47
Sok, Baron		610	1.0978	0.45	1.0	1.8		1.85
Brown		350	0.0518	0.88	1.0	2.9		2.56
Shah		700	0.64	0.2	1.0	1.4		1.45
Entov	1	580	0.65	0.3	1.0	1.5		1.59
	2	580	0.273	0.65	1.0	1.5		1.94

considered to be correlated by the theory to separately measured values of the strength of concrete and to the maximum aggregate size, which limited the freedom in fitting test data. Without these limitations, still smaller coefficients of variation could be achieved with Bažant's and Oh's [28] model.

Stimulated by the present work, the practical fracture analysis of concrete with the R-curve approach has been subsequently investigated by Bažant and Cedolin [36], who introduce for the R-curve, instead of a differential equation (Eq. 21), a simple algebraic formula with parameters related to concrete strength and aggregate size, but independent of body geometry and the location of loading points. Using solutions of linear elastic fracture mechanics, they demonstrate good agreement with typical maximum load data from fracture tests of concrete. The coefficient of variation of errors is about the same as here, and the same as in Ref. [29], which confirms that the errors are due mainly to the randomness of material behavior rather than the method of analysis.

Conclusion

Good agreement with available fracture test data for concrete may be obtained if the crack length dependence of the energy consumed per unit fracture extension is calculated for an infinite elastic medium loaded at infinity and if this energy is matched to that indicated for the actual body geometry by a linear elastic fracture mechanics solution for an effective crack length. The concept of energy separation rate associated with a finite crack growth step, and the assumption of uniform tensile stress within the nonlinear zone ahead of the fracture front, yield realistic R-curves.

Acknowledgment

The work was sponsored under U.S. National Science Foundation Grant No. CEE800-9050 to Northwestern University, directed by Z.P. Bažant. M.P. Wnuk, Visiting Professor at Northwestern University, and Edward Law appreciate financial support under this grant. Mary Hill is to be thanked for her excellent secretarial assistance.

Appendix A. Solutions of boundary value problem and derivation of Eq. (15)

Sneddon (40) considered an integral transform approach to a boundary value problem involving a two-dimensional stress field generated around a Griffith crack. In particular, he obtained an integral representation for the opening displacement as a function of location, $u_y = u_y(\bar{x}, \bar{y})$. Within the crack plane ($\bar{y} = 0$), Sneddon's formula reads

$$\left[u_y(x, y)\right]_{y=0} = \frac{4l}{\pi E_1} \int_x^1 \frac{t\,\mathrm{d}t}{\sqrt{t^2 - x^2}} \int_0^t \frac{p(u)\,\mathrm{d}u}{\sqrt{t^2 - u^2}}. \tag{A1}$$

Here, $E_1 = E$ for plane stress, $E_1 = E(1 - \nu^2)^{-1}$ for plane strain; l denotes the half-length of the crack, and x, u and y are nondimensional variables

$$x = \bar{x}/l, \qquad u = \bar{u}/l, \qquad y = \bar{y}/l. \tag{A2}$$

Symbol $p(u)$ denotes the pressure exerted directly on the crack surface. For the fictitious crack model, in which the crack is extended by an additional cut from $\bar{x} = a$ to $\bar{x} = a + R$, the length l should be replaced by $a + R$, in which a denotes the half-length of the actual crack, while R is the length of the end zone adjacent to the crack, see Fig. A1. Pressure p is given in terms of the remotely applied stress σ and the restraining stress $S(x)$, defined over the end zone $a < \bar{x} \le a + R$, as follows (see Fig. A1):

$$p(\bar{x}) = \begin{cases} \sigma, & 0 \le \bar{x} \le a, \\ \sigma - S(\bar{x}), & a < \bar{x} \le a + R \end{cases} \tag{A3}$$

or

$$p(x) = \begin{cases} \sigma, & 0 \le x \le m, \\ \sigma - S(x), & m < x < 1. \end{cases} \tag{A4}$$

Here we consider a restraining stress S which falls off from the maximum value σ_0, attained at $\bar{x} = a + R$,

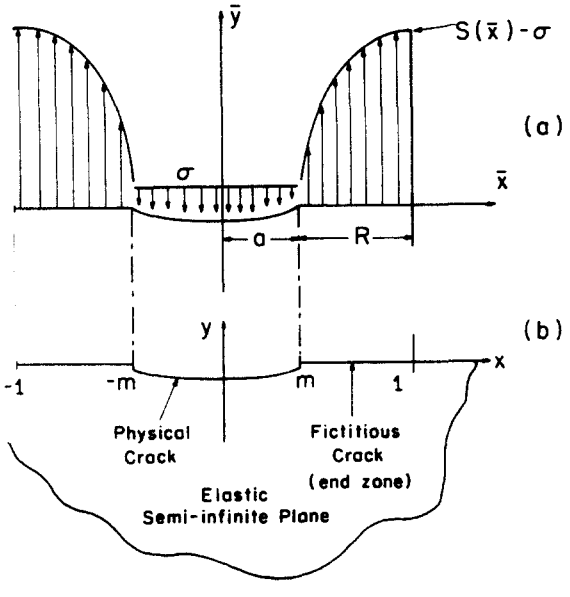

Fig. A1. Assumed distribution of stresses on the surface of an extended crack.

to zero at the crack tip, $\bar{x} = a$, i.e.,

$$S(\bar{x}) = \frac{\sigma_0}{R}(\bar{x} - a), \quad a \le \bar{x} \le a + R. \tag{A5}$$

Introducing the nondimensional quantities

$$m = a/(a+R), \qquad x = \bar{x}/(a+R) \tag{A6}$$

we rewrite equations (A4) and (A5) in the following way:

$$S(x) = \frac{\sigma_0}{1-m}(x-m), \quad m \le x \le 1,$$

$$p(x) = \begin{cases} \sigma, & 0 \le x \le m, \\ \sigma - \sigma_0 \dfrac{x-m}{1-m}, & m < x \le 1. \end{cases} \tag{A7}$$

Let us now evaluate the integrals involved in the Sneddon's representation of the opening displacement given by Eq. (A1). Denoting the inner integral by $f(t)$, we have

$$f(t) = \int_0^t \frac{p(u)\,\mathrm{d}u}{\sqrt{t^2-u^2}} = \begin{cases} \displaystyle\int_0^t \frac{\sigma\,\mathrm{d}u}{\sqrt{t^2-u^2}} = f_1(t), & 0 \le t \le m, \\ \displaystyle\int_0^m \frac{\sigma\,\mathrm{d}u}{\sqrt{t^2-u^2}} + \int_m^t \frac{\sigma - S(u)}{\sqrt{t^2-u^2}}\,\mathrm{d}u = f_2(t), & m < t \le 1. \end{cases} \tag{A8}$$

To obtain the information pertinent to the essential work of fracture $\mathscr{G}^{\Delta}$, we need to investigate in detail the displacement u_y within the end zone, that is, for $m < t \le 1$. With the notation defined by Eq. (A8), Eq. (A1) reduces to

$$[u_y]_{y=0} = \frac{4(a+R)}{\pi E_1} \begin{cases} \displaystyle\int_x^1 \frac{t f_1(t)\,\mathrm{d}t}{\sqrt{t^2-x^2}}, & 0 \le x \le m, \\ \displaystyle\int_x^1 \frac{t f_2(t)\,\mathrm{d}t}{\sqrt{t^2-x^2}}, & m < x \le 1. \end{cases} \tag{A9}$$

The second equation in (A9) is of particular interest. Let us first evaluate the auxiliary function

$$\begin{aligned} f_2(t) &= \int_0^m \frac{\sigma\,\mathrm{d}u}{\sqrt{t^2-u^2}} + \int_m^t \frac{\sigma - \sigma_0\left(\dfrac{u-m}{1-m}\right)}{\sqrt{t^2-u^2}}\,\mathrm{d}u = \int_0^t \frac{\sigma\,\mathrm{d}u}{\sqrt{t^2-u^2}} - \frac{\sigma_0}{1-m}\int_m^t \frac{u-m}{\sqrt{t^2-u^2}}\,\mathrm{d}u \\ &= \left[-\sigma \cos^{-1}\left(\frac{u}{t}\right)\right]_0^t + \frac{\sigma_0 m}{1-m}\left[\cos^{-1}\left(\frac{u}{t}\right)\right]_m^t - \frac{\sigma_0}{1-m}\int_m^t \frac{u\,\mathrm{d}u}{\sqrt{t^2-u^2}} \\ &= \sigma\frac{\pi}{2} + \frac{m\sigma_0}{1-m}\cos^{-1}\left(\frac{m}{t}\right) - \frac{\sigma_0\sqrt{t^2-m^2}}{1-m}. \end{aligned} \tag{A10}$$

Substituting this last expression for $f_2(t)$ into the second equation in (A9), we obtain, for $m < x < 1$,

$$\begin{aligned} [u_y]_{y=0} = \frac{4(a+R)}{\pi E_1}\Bigg\{ &\frac{\pi}{2}\sigma\int_x^1 \frac{t\,\mathrm{d}t}{\sqrt{t^2-x^2}} + \frac{m\sigma_0}{1-m}\int_x^1 \frac{t\cos^{-1}(m/t)\,\mathrm{d}t}{\sqrt{t^2-x^2}} \\ &- \frac{\sigma_0}{1-m}\int_x^1 \sqrt{\frac{t^2-m^2}{t^2-x^2}}\,t\,\mathrm{d}t\Bigg\}. \end{aligned} \tag{A11}$$

The first integral in the braces is elementary while the second one may be evaluated by parts.

$$\int_x^1 \frac{\cos^{-1}(m/t)}{\sqrt{t^2-x^2}}\, t\, \mathrm{d}t = \left[\sqrt{t^2-x^2}\, \cos^{-1}\left(\frac{m}{t}\right)\right]_x^1 - \int_x^1 \frac{\sqrt{t^2-x^2}}{\sqrt{1-(m/t)^2}}\,(m/t^2)\, \mathrm{d}t$$

$$= \sqrt{1-x^2}\, \cos^{-1} m - m\int_x^1 \sqrt{\frac{t^2-x^2}{t^2-m^2}}\, \frac{\mathrm{d}t}{t}. \tag{A12}$$

Now we have $(m < x < 1)$

$$[u_y]_{y=0} = \frac{4(a+R)\sigma_0}{\pi E_1}\left\{Q\sqrt{1-x^2} + \frac{m}{1-m}\left[\sqrt{1-x^2}\, \cos^{-1} m - m\int_x^1 \sqrt{\frac{t^2-x^2}{t^2+m^2}}\, \frac{\mathrm{d}t}{t}\right]\right.$$

$$\left. - \frac{1}{1-m}\int_x^1 \sqrt{\frac{t^2-m^2}{t^2-x^2}}\, t\, \mathrm{d}t\right\}$$

$$= \frac{4\sigma_0 R}{\pi E_1}\left(\frac{a+R}{R}\right)\left\{\left(Q + \frac{m}{1-m}\, \cos^{-1} m\right)\sqrt{1-x^2}\right.$$

$$\left. - \frac{1}{1-m}\int_x^1 \left[\sqrt{\frac{t^2-x^2}{t^2-m^2}}\, \frac{m^2}{t} + \sqrt{\frac{t^2-m^2}{t^2-x^2}}\, t\right] \mathrm{d}t\right\}. \tag{A13}$$

It remains to evaluate the integral

$$I = \int_x^1 \left[\sqrt{\frac{t^2-x^2}{t^2-m^2}}\, \frac{m^2}{t} + \sqrt{\frac{t^2-m^2}{t^2-x^2}}\, t\right] \mathrm{d}t = \int_x^1 \frac{m^2t^2 - m^2x^2 + (t^2-m^2)t^2}{t\sqrt{(t^2-m^2)(t^2-x^2)}}\, \mathrm{d}t$$

$$= \int_x^1 \frac{(-m^2x^2 + t^4)\, \mathrm{d}t}{t\sqrt{(t^2-m^2)(t^2-x^2)}}. \tag{A14}$$

With $t^2 = z$ this last integral becomes

$$I = -m^2x^2\int_{x^2}^1 \frac{\mathrm{d}z}{z\sqrt{(z-m^2)(z-x^2)}} + \int_{x^2}^1 \frac{z\, \mathrm{d}z}{\sqrt{(z-m^2)(z-x^2)}} \tag{A15}$$

or, concisely,

$$I = -mx^2 I_1 + I_2. \tag{A16}$$

The integrals I_1 and I_2 can be evaluated in a closed form. After a number of algebraic operations the results are

$$I_1 = \frac{1}{mx}\log\frac{x/m + \sqrt{(1-x^2)/(1-m^2)}}{x/m - \sqrt{(1-x^2)/(1-m^2)}},$$

$$I_2 = \sqrt{(1-m^2)(1-x^2)} + \frac{m^2+x^2}{2}\log\frac{1+\sqrt{(1-x^2)/(1-m^2)}}{1-\sqrt{(1-x^2)/(1-m^2)}}. \tag{A17}$$

Combining these results with (A15-A16) and replacing $[Q + (m/1-m)\cos^{-1} m]$ by $[(1+m)/(1-m)]^{1/2}$ in

Eq. (A13), [1] we obtain the final expression for the opening displacement ($m \le x \le 1$):

$$[u_y]_{y=0} = \frac{4\sigma_0 R}{\pi E_1} \frac{a+R}{4R(1-m)} \left\{ 2\sqrt{(1-m^2)(1-x^2)} - 2mx \log \frac{1+mx+\sqrt{(1-m^2)(1-x^2)}}{1+mx-\sqrt{(1-m^2)(1-x^2)}} \right.$$

$$\left. -(x-m)^2 \log \frac{\sqrt{1-m^2}+\sqrt{1-x^2}}{\sqrt{1-m^2}-\sqrt{1-x^2}} \right\}. \tag{A18}$$

For simplicity, denote $4\sigma R/\pi E_1$ by C and let

$$\sqrt{1-m^2} = M, \qquad \sqrt{1-x^2} = X. \tag{A19}$$

Since $m = a/(a+R)$, we see that $(a+R)/R = (1-m)^{-1}$. Therefore, Eq. (A18) may be briefly written in the form ($m \le x \le 1$)

$$[u_y]_{y=0} = \frac{C}{4(1-m^2)} \left\{ 2MX - 2mx \log \frac{1+mx+MX}{1+mx-MX} - (x-m)^2 \log \frac{M+X}{M-X} \right\}. \tag{A20}$$

So far we did not restrict the quantity m in any way, and thus the formula for the opening displacement (A20) remains valid for an arbitrary ratio R/a. This means that Eq. (A20) holds for both the large scale yielding and the small scale yielding situations.

Since the tip opening displacement (u_{tip}) is directly proportional to the J-integral, it is of interest to provide an expression for u_{tip} which would be valid for a large scale yielding situation. This expression results from Eq. (A20) when x is set equal to m. We have then

$$u_{tip} = \frac{C}{4(1-m^2)} \left[2(1-m^2) + 4m^2 \log m \right]. \tag{A21}$$

Returning to the dimensional quantities R and a, we may rewrite this equation as

$$u_{tip} = \frac{4\sigma_0}{\pi E_1} a \left[1 + \frac{R}{2a} - \frac{a}{R} \log\left(1 + \frac{R}{a}\right) \right]. \tag{A22}$$

For brittle fracture, however, it is appropriate to assume that the length of the end zone is small compared to the crack length. In this case the ratio R/a approaches zero and this implies $m \to 1$. Treating the quantity $\varepsilon = 1 - m$ as a small parameter and expanding all terms in Eq. (A20) into a power series of ε we reduce the lengthy expression (A20) to the following form ($m \le x \le 1$):

$$[u_y]_{y=0} = C \left\{ \left(1 - \frac{\xi}{2}\right)\sqrt{1-\xi} - \frac{\xi^2}{4} \log \frac{1+\sqrt{1-\xi}}{1-\sqrt{1-\xi}} - \tfrac{1}{3}(1-\xi)^{2/3}\varepsilon + \cdots \right\}. \tag{A23}$$

Here ξ denotes a distance x_1 measured from the tip of the actual crack, normalized by the length of the end zone, i.e.,

$$\xi = \frac{x_1}{R} = \frac{x-m}{1-m}. \tag{A24}$$

[1] It should be noted that the load Q and the size m of the end zone are not independent. The finiteness condition established for an extended crack requires that the applied load σ and the length of the end section R are related in a certain manner. This relation ensues when the K-factor defined by Eq. (2.1) is set to zero. We obtain then $\sigma = (2/\pi)\int_m^1 S(x)(1-x^2)^{-1/2}\,dx$. Substituting (A4) for the distribution $S(x)$ and carrying out the integrals involved, we obtain $Q = [(1-m)/(1+m)]^{1/2} - [m/(1-m)]\cos^{-1} m$, in which $Q = \pi\sigma/2\sigma_0$. This equation applies for the specific type of the restraining stress distribution considered here, i.e., $S(x) = \sigma_0(x-a)/R$.

If only the term of the zero order, contained in the square bracket, is retained, we have

$$\left[u_y(x_1, R)\right]_{ssy} = \frac{4\sigma_0 R}{\pi E_1}\left\{\left(1-\frac{x_1}{2R}\right)\sqrt{1-\frac{x_1}{R}} - \frac{x_1^2}{4R^2}\log\frac{1+\sqrt{1-x_1/R}}{1-\sqrt{1-x_1/R}}\right\}. \tag{A25}$$

where the subscript ssy refers to small scale yieldings. We may note now that Eq. (A25) is identical with Eq. (15) used in the text. It is readily seen that when the distance x_1 is set to zero in (A25), we obtain the tip displacement

$$u_{tip} = (4\sigma_0/\pi E_1)R. \tag{A26}$$

This formula is in accordance with Eq. (A22), quoted earlier, since when $R/a \ll 1$, we may use the expansions

$$\log\left(1+\frac{R}{a}\right) = \frac{R}{a} - \tfrac{1}{2}\left(\frac{R}{a}\right)^2 + \cdots, \qquad -\frac{a}{R}\log\left(1+\frac{R}{a}\right) = -1 + \tfrac{1}{2}\frac{R}{a} + \cdots \tag{A27}$$

which reduce (A22) to (A26).

Appendix B. Reduction of essential work criterion to final stretch condition

Evaluation of the energy separation rate $\mathscr{G}^{\Delta}$ involves an integration of the product of the restraining stress S and the crack opening δu_y associated with an incremental crack extension, δa. Rewriting Eq. (17) we have

$$\mathscr{G}^{\Delta} = -2\int_0^{\Delta} S(x_1)\delta u_y(x_1). \tag{B1}$$

Here we have replaced the variable x, present in Eq. (17), by the distance measured from the crack tip x_1. The minus sign in Eq. (B1) is added to account for the fact that the work that is being computed is done against the restraining stress (stress and the displacement vectors are at 180° to each other). This renders the integral $\int_0^{\Delta} S(x_1)\delta u_y(x_1)$ negative, while we would like to have a positive energy separation rate $\mathscr{G}^{\Delta}$. Note also that if the control point at which work $\mathscr{G}^{\Delta}$ is evaluated is considered stationary while the crack front approaches, the distance x_1 may be treated as a timelike variable, $x_1 = x_1(t)$, just as the current crack half-length was in the previous formulation. Since the relation between a and x_1 is $a + x_1 = x$, and since x is constant, we also have

$$da = -dx_1, \qquad \partial/\partial a = -\partial/\partial x_1. \tag{B2}$$

From $\delta u_y = u_y(x_1, a+\delta a) - u_y(x, a)$ we get

$$\delta u_y = u_y(x, a+\delta a) - u_y(x, a) = \frac{\partial u_y}{\partial a}\delta a. \tag{B3}$$

Replacing a by the time-like variable x_1, and employing Eq. (B2), we have

$$\delta u_y = \frac{\partial u_y}{\partial x_1}\, dx_1. \tag{B4}$$

With this expression, integral (B1) becomes

$$\mathscr{G}^{\Delta} = -2\int_0^{\Delta} S(x_1)\frac{\partial u_y(x_1)}{\partial x_1}\, dx_1. \tag{B5}$$

We will prove that, for certain types of the distribution of the restraining stress, the integral in (B5)

reduces to an expression involving the *difference* between the crack opening displacement at the point coinciding with the current crack tip (instant t_2) and the crack opening displacement (COD) that existed at this point at the instant just prior to collapse of the process zone associated with the crack of length a (instant t_1). It is easily seen that the two values of the variable x_1 which correspond to these two instances are

$$\begin{aligned} &x_1 = \Delta \quad \text{at } t = t_1, \quad \text{crack length} = a, \\ &x_1 = 0 \quad \text{at } t = t_2, \quad \text{crack length} = a + \Delta. \end{aligned} \tag{B6}$$

If the notation $u_y = u_y(x_1, a)$ is adopted, then the crack opening displacements evaluated at the same control point P (Fig. B1), but corresponding to the two instances, may be written as

$$\begin{aligned} &u_y(\Delta, a) \qquad \text{at instant } t_1, \\ &u_y(0, a + \Delta) \quad \text{at instant } t_2. \end{aligned} \tag{B7}$$

Next, we may consider two cases:

(a) constant restraining stress, $S = \sigma_0$, over the entire end zone, and

(b) restraining stress which falls off in a linear fashion from a maximum value, σ_0, at the outer edge of the end zone, to zero at the current crack tip, i.e.,

$$S(x_1) = \frac{x_1}{R}\sigma_0, \quad 0 \le x_1 \le R. \tag{B8}$$

For the first case we have

$$\mathcal{G}^{\Delta} = -2\sigma_0 \int_{u_y(0,\, a+\Delta)}^{u_y(\Delta,\, 0)} \delta u_y = 2\sigma_0 \left[u_y(0, a + \Delta) - u_y(\Delta, a) \right]. \tag{B9}$$

Setting this quantity equal to the essential work of fracture

$$\hat{\mathcal{G}} = \sigma_0 \hat{\delta} \tag{B10}$$

(in which $\hat{\delta}$ denotes the final stretch) reduces the energy criterion of fracture, $\mathcal{G}^{\Delta} = \hat{\mathcal{G}}$, to the final stretch condition, namely,

$$u_y(0, a + \Delta) - u_y(\Delta, a) = \hat{\delta}/2. \tag{B11}$$

It may be noted that the quantities $\hat{\mathcal{G}}$ and $\hat{\delta}$ are material characteristics while the quantity $\mathcal{G}^{\Delta}$ measures the intensity of the near-tip stress field and results from a solution of an appropriate boundary value problem involving a crack modified by an assumption concerning the type of the S-stress distribution (which is not included in the continuum treatment of the problem).

For the second case, which is that of a restraining stress decreasing linearly from σ_0 to zero over length R, we note

$$S(0) = 0, \qquad S(\Delta) = (\Delta/R)\sigma_0, \qquad \mathrm{d}S/\mathrm{d}x_1 = \sigma_0/R. \tag{B12}$$

Using these properties and integrating the integral in Eq. (B1) by parts, we obtain

$$\begin{aligned} \mathcal{G}^{\Delta} &= \left[-2u_y(x_1) S(x_1) \right]_0^{\Delta} + 2\int_0^{\Delta} u_y(x_1) \frac{\mathrm{d}S(x_1)}{\mathrm{d}x_1}\, \mathrm{d}x_1 \\ &= 2\left\{ -\frac{\Delta}{R}\sigma_0 u_y(\Delta) + \frac{\sigma_0}{R}\int_0^{\Delta} u_y(x_1)\, \mathrm{d}x_1 \right\} = 2\sigma_0 \frac{\Delta}{R}\left\{ -u_y(\Delta) + \frac{1}{\Delta}\int_0^{\Delta} u_y(x_1)\, \mathrm{d}x_1 \right\}. \end{aligned} \tag{B13}$$

This is as far as we can go without making any simplifications. However, the quantity $\Delta^{-1}\int_0^{\Delta} u_y(x_1)\mathrm{d}x_1$ can

be approximated by the mean value of function $u_y(x_1)$ over interval $0 \le x_1 \le \Delta$, i.e.,

$$\frac{1}{\Delta}\int_0^{\Delta} u_y(x_1)\,\mathrm{d}x_1 \approx \frac{u_y(0)+u_y(\Delta)}{2}. \tag{B14}$$

With this, expression (B13) becomes

$$\mathscr{G}^{\Delta} = 2\sigma_0 \frac{\Delta}{R}\left\{\frac{u_y(0)-u_y(\Delta)}{2}\right\}. \tag{B15}$$

Consider now the work done on a material element located at some control point P while the stress at this point is being gradually released from the value $(\Delta/R)\sigma_0$ to zero when the crack front reaches point P. Since the time interval involved $(t_2 - t_1 = \delta t = \Delta/\dot{a})$ is small, we may consider the motion of the crack front to be uniform during such incremental crack extension. This implies a variation of stress at P which is linear with time. Thus, if the final displacement increment attained during the time interval δt is denoted by $\hat{\delta}$ (final stretch), the work done is

$$\hat{\mathscr{G}} = \tfrac{1}{2}\left(\sigma_0 \frac{\Delta}{R}\right)(\hat{\delta}). \tag{B16}$$

This is the so-called essential work of fracture. To make an extension of fracture possible, the energy $\hat{\mathscr{G}}$ has to be continually supplied from the near-tip stress field. When the expressions (B15) and (B16) are equated, and when it is recalled that $u_y(0)$ is in fact $u_y(0, a+\Delta)$ while $u_y(\Delta)$ is $u_y(\Delta, a)$, we again recover the final stretch condition (B11) which describes the stable phase of crack extension.

Appendix C. *R*-curve equation based on final stretch concept. Derivation of Eq. (21).

As shown in Appendix A, the displacement normal to the crack plane occurring within the end zone, $0 \le x_1 \le R$, is obtained by a continuum mechanics approach with a non-continuum type of stress incorporated into the modified boundary condition for an extended crack (Fig. A1). The final result may be represented in the form

$$[u_y]_{y=0,\,0\le x_1\le R} = \left(\frac{4\sigma_0}{\pi E_1}\right) R f\left(\frac{x_1}{R}\right). \tag{C1}$$

For a moving stable crack, the extent of the nonlinear zone (R) varies with the crack length (a), and so one must regard R as a certain, a priori unknown, function of a. Examples of specific forms of expression (C1) are provided by Eqs. (13) (14) and (15). In what follows we assume that the solution of the field problem, of the type of Eq. (C1), is known. The objective is to employ the form (C1) in order to derive an equation which would define the R-curve. Although the J-integral is a commonly used measure of the apparent material resistance to stable cracking, we may equally well employ the length of the end zone, R, as such measure. Indeed, within the small scale yielding range discussed here both measures are equivalent. Therefore, we seek to determine the function

$$R = R(a). \tag{C2}$$

As will be shown, a certain nonlinear differential equation may be derived for $R(a)$.

An incremental change in the material resistance to cracking, $\mathrm{d}R$, may be related to the increment of crack growth, $\mathrm{d}a$, through the application of the fracture criterion based on the final stretch concept, see Eq. (B11). The quantities $u_y(0, a+\Delta)$ and $u_y(\Delta, a)$ entering into this criterion are evaluated from Eq. (C1) as follows:

$$\begin{aligned} u_y(0, a+\Delta) &= (4\sigma_0/\pi E_1) R(a+\Delta), \\ u_y(\Delta, a) &= (4\sigma_0/\pi E_1) R(a) f[x_1/R(a)]. \end{aligned} \tag{C3}$$

Replacing $R(a+\Delta)$ by the first two terms of the Taylor series expansion, $R(a)+\Delta\, dR/da$, and employing Eq. (B11), we obtain

$$\frac{\hat{\delta}}{2}=\frac{4\sigma_0}{\pi E_1}\left\{R(a)+\Delta\frac{dR}{da}-R(a)f[\Delta/R(a)]\right\}. \tag{C4}$$

This equation may be used in two different ways. First, it can be applied to define the energy separation rate $\mathcal{G}^{\Delta}$, which is given by the integral (B1), namely

$$\mathcal{G}^{\Delta}=\frac{8\sigma_0^2}{\pi E_1}\left\{R+\Delta\frac{dR}{da}-Rf(\Delta/R)\right\}, \tag{C5}$$

where R briefly stands for $R(a)$. Secondly, Eq. (C4) may be used for solving for the rate of change of the apparent material toughness, that is,

$$\frac{dR}{da}=\left(\frac{\pi E_1}{8\sigma_0}\right)\left(\frac{\hat{\delta}}{\Delta}\right)-\frac{R}{\Delta}+\frac{R}{\Delta}f\left(\frac{\Delta}{R}\right). \tag{C6}$$

When the group of material constants appearing on the right-hand side of this equation is identified with the *tearing modulus*, M, the form (6) becomes identical with Eq. (21) used in the text to define an R-curve. This is so for a constant restraining stress, while for a linearly varying restraining stress Eq. (C6) combined with Eq. (A25) yields

$$\frac{dR}{da}=M-\frac{R}{\Delta}+\left(1-\frac{\Delta}{2R}\right)\sqrt{\frac{R}{\Delta}\left(\frac{R}{\Delta}-1\right)}-\frac{\Delta}{4R}\log\frac{\sqrt{R/\Delta}+\sqrt{(R/\Delta)-1}}{\sqrt{R/\Delta}-\sqrt{(R/\Delta)-1}}. \tag{C7}$$

Examples of the R-curves which resulted from numerical integration of Eqs. (21) and (C7), both of which are special cases of Eq. (C6), are shown in Fig. 3. It should be emphasized that a different R-curve is obtained each time when the basic assumption regarding the distribution of the restraining stresses is changed. Since each time a new boundary value problem has to be solved, a new function $f(\Delta/R)$ is generated. This fact is reflected by the presence of the function $f(\Delta/R)$ in the governing Eq. (C6).

It may be demonstrated, however, that large variations in the S-stress distribution have only minor effect on the final shape of the R-curve, see for instance Fig. 3. To illuminate this point, consider a limiting case of $R\approx\Delta$ when both equations defining the resistance curve, i.e., Eqs. (21) and (C7), reduce to simple asymptotic forms which differ only insignificantly,

$$\frac{dR}{da}\simeq\begin{cases}M-\rho+\frac{2}{3}\dfrac{(\rho-1)^{3/2}}{\rho^{1/2}}, & \rho\to 1,\quad \text{constant } S, \qquad \text{(C8a)}\\[2ex] M-\rho+\frac{4}{3}\dfrac{(\rho-1)^{3/2}}{\rho^{1/2}}, & \rho\to 1,\quad \text{linear } S. \qquad \text{(C8b)}\end{cases}$$

These equations describe the R-curve for the limiting case of brittle fracture, when the ductility parameter $\rho=R/\Delta$ approaches one.

Contrasting with this observation is the substantial effect of the initial condition on the shape of an R-curve. The value of the material toughness at the onset of crack growth, R_{ini}, and in particular the ratio of R_{ini} to the process zone size (or the growth step Δ) has a distinct effect on the slope of R-curve, and consequently, on the occurrence of stable-unstable transition in the mode of fracture propagation (compare the curves shown in Figs. 4 and 5).

Appendix D. LEFM K-factors and compliances for fracture specimens

1. Single-edge notch (SEN) tensile specimen

According to the Tada–Paris–Irwin manual [39], the stress intensity factor is

$$K = \sigma\sqrt{a}\,\phi\left(\frac{a}{b}\right), \qquad \phi\left(\frac{a}{b}\right) = \sqrt{\pi}\,f_1\left(\frac{a}{b}\right) f_2\left(\frac{a}{b}\right), \qquad \sigma = \frac{P}{bB}, \tag{D1}$$

in which P denotes the applied load, remote from the crack plane, a is the crack length, b is specimen width, B is its thickness, and

$$f_1\left(\frac{a}{b}\right) = \left\{\frac{2b}{\pi a}\tan\left(\frac{\pi a}{2b}\right)\right\}^{1/2},$$

$$f_2\left(\frac{a}{b}\right) = \frac{.752 + 2.02(a/b) + .37[1 - \sin(\pi a/2b)]^3}{\cos(\pi a/2b)}. \tag{D2}$$

The accuracy of these expressions is better than 0.5% for an arbitrary a/b ratio. If we denote a/b by α and $\pi a/2b$ by α_1, then

$$\frac{d\phi}{d\alpha} = \sqrt{\pi}\left(\frac{\pi}{2}\right)\frac{f_2}{f_1}\,\frac{\alpha_1 - \frac{1}{2}\sin 2\alpha_1}{\alpha_1^2\cos^2\alpha_1} + \sqrt{\pi}\,f_1\left[\frac{2.02}{\cos\alpha_1} - \sqrt{\pi}\,(1 - \sin\alpha_1)^2 + f_2\tan\alpha_1\right]. \tag{D3}$$

In order to determine the compliance function, $C = C(a/b)$, we consider the displacement at distance h from the crack plane,

$$\delta_{tot} = \delta_{no\ crack} - \delta_{crack},$$

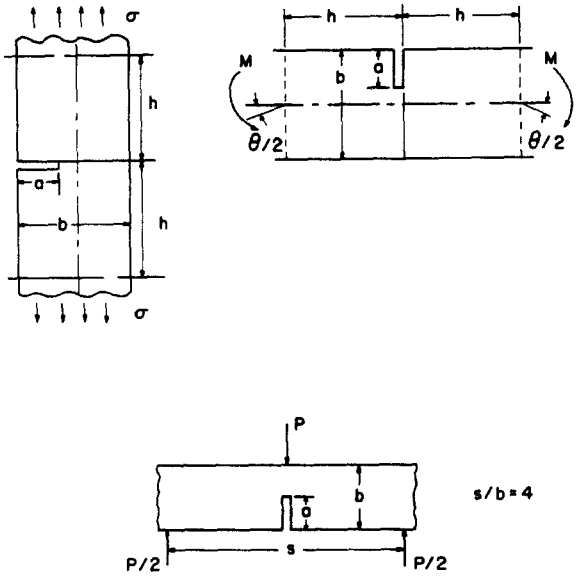

Fig. D1. Common geometries of specimens used to test fracture behavior of structural materials.

in which

$$\delta_{\text{no crack}} = \left[\frac{\sigma}{E}(2h)\right]_{h=2b} = \frac{4\sigma b}{E},$$
$$\delta_{\text{crack}} = \frac{4\sigma a}{E}\frac{(a/b)}{1-(a/b)^2}\left\{0.99 - \frac{a}{b}\left(1-\frac{a}{b}\right)\left[1.3 - 1.2\frac{a}{b} + 0.7\left(\frac{a}{b}\right)^2\right]\right\}. \tag{D4}$$

Then $C(a/b) = \delta_{\text{tot}}/P$, i.e.,

$$C\left(\frac{a}{b}\right) = \kappa\left\{\frac{\alpha^2}{1-\alpha^2}\left[.99 - \alpha(1-\alpha)(1.3 - 1.2\alpha + 0.7\alpha^2)\right] + 1\right\}, \tag{D5}$$

where $\kappa = 4\sigma b/E$. In a nondimensional form we have

$$Z\left(\frac{a}{b}\right) = \kappa^{-1}C\left(\frac{a}{b}\right) = \frac{\alpha^2}{1-\alpha^2}\left[0.99 - \alpha(1-\alpha)(1.3 - 1.2\alpha + 0.7\alpha^2)\right] + 1. \tag{D6}$$

The derivative $dZ/d\alpha$ becomes

$$\frac{dZ}{d\alpha} = \frac{2\alpha}{(1-\alpha^2)^2}\left[0.99 - \alpha(1-\alpha)(1.3 - 1.2\alpha + 0.7\alpha^2)\right] + \frac{\alpha^2}{1-\alpha^2}\left[-1.3 + 2.6\alpha - 5.7\alpha^2\right]. \tag{D7}$$

b. Three-point bent specimen

According to the Tada–Paris–Irwin handbook [39]

$$K = \sigma\sqrt{\pi a}\left[1.090 - 1.735\left(\frac{a}{b}\right) + 8.20\left(\frac{a}{b}\right)^2 - 14.18\left(\frac{a}{b}\right)^3 + 14.57\left(\frac{a}{b}\right)^4\right], \tag{D8}$$

where $\sigma = 6M/b^2B$, $M = Ps/4$, provided that $0 \le a/b \le 0.6$. In this range, the accuracy of Eq. (D8) is better than 0.2%. The nondimensional ϕ-factor and its derivative are given by

$$\phi = \sqrt{\pi}\,(1.090 - 1.735\alpha + 8.20\alpha^2 - 14.18\alpha^3 + 14.57\alpha^4), \tag{D9}$$

$$\frac{d\phi}{d\alpha} = \sqrt{\pi}\,(-1.735 + 16.4\alpha - 42.54\alpha^2 + 52.28\alpha^3). \tag{D10}$$

The deflection at the point of load application is $\delta_{\text{tot}} = \delta_{\text{no crack}} + \delta_{\text{crack}}$ in which

$$\delta_{\text{no crack}} = \frac{8}{9}\left(\frac{3s^2P}{2Eb^2B}\right), \tag{D11}$$

$$\delta_{\text{crack}} = \kappa_1\left(\frac{\alpha}{1-\alpha}\right)^2(5.58 - 19.57\alpha + 36.82\alpha^2 - 34.94\alpha^3 + 12.77\alpha^4). \tag{D12}$$

When the constant $\kappa_1 = (93s^2P/2Eb^2B)$ is factored out,

$$\delta_{\text{tot}} = \kappa_1\left[\left(\frac{\alpha}{1-\alpha}\right)^2 F(\alpha) + \tfrac{8}{9}\right] \tag{D13}$$

in which $F(\alpha) = 5.58 - 19.57\alpha + 36.82\alpha^2 - 34.94\alpha^3 + 12.77\alpha^4$. This form indicates a nondimensional compliance function

$$Z(a/b) = \kappa_1^{-1}C(a/b) = \left(\frac{\alpha}{1-\alpha}\right)^2 F(\alpha) + \tfrac{8}{9}. \tag{D14}$$

Hence we find the derivative

$$\frac{dZ}{d\alpha}=\left(\frac{\alpha}{1-\alpha}\right)^2\left[\frac{2F(\alpha)}{\alpha(1-\alpha)}+\frac{dF}{d\alpha}\right],\quad \frac{dF}{d\alpha}=-19.57+73.64\alpha-104.82\alpha^2+51.08\alpha^3. \tag{D15}$$

c. Four-point bent configuration

The Tada–Paris–Irwin handbook [39] indicates, without any restrictions on the a/b ratio,

$$K=\sigma\sqrt{\pi a}\,F_1\left(\frac{a}{b}\right)\left[0.923+0.199F_2\left(\frac{a}{b}\right)\right],\quad \sigma=\frac{6M}{b^2B}, \tag{D16}$$

in which

$$F_1(\alpha_1)=\frac{1}{\cos\alpha_1}\sqrt{\frac{\tan\alpha_1}{\alpha_1}},\qquad F_2(\alpha_1)=(1-\sin\alpha_1)^4,\quad \alpha_1=\frac{\pi a}{2b}. \tag{D17}$$

Accuracy of this formula is better than 0.5% for any a/b, while the accuracy of the expressions for the compliance function (which follow) is better than 1% for any a/b. From Eq. (D16)

$$\frac{d\phi}{d\alpha}=\left(\frac{\pi}{2}\right)\sqrt{\pi}\left[\frac{dF_1}{d\alpha_1}(0.923+0.199F_2)+0.199F_1\frac{dF_2}{d\alpha_1}\right] \tag{D18}$$

in which

$$\frac{dF_1}{d\alpha_1}=\sqrt{\frac{x_1}{\tan\alpha_1}}\,\frac{\alpha_1-\frac{1}{2}\sin(2\alpha_1)+2\alpha_1\sin^2\alpha_1}{2\alpha_1^2\cos^3\alpha_1},\qquad \frac{dF_2}{d\alpha_1}=-4(\cos\alpha_1)(1-\sin\alpha_1)^3. \tag{D19}$$

The compliance of a four-point bent specimen is defined as a reciprocal of the ratio of the moment M and the relative angle of rotation of two cross sections located symmetrically a certain distance h from the crack plane (we assume $h=2b$), namely, $\theta_{tot}=\theta_{no\ crack}+\theta_{crack}$, in which

$$\theta_{no\ crack}=\left[\frac{24M}{Eb^2B}\left(\frac{h}{b}\right)\right]_{h=2b}=\frac{48M}{Eb^2B},\qquad \theta_{crack}=\frac{24M}{Eb^2B}\left(\frac{\alpha}{1-\alpha}\right)^2G(\alpha), \tag{D20}$$

$$G(\alpha)=5.93-19.69\alpha+37.14\alpha^2-35.84\alpha^3+13.12\alpha^4. \tag{D21}$$

Therefore, the compliance assumes the form

$$C\left(\frac{a}{b}\right)=\frac{\theta_{tot}}{M}=\frac{24}{Eb^2B}\left[\left(\frac{\alpha}{1-\alpha}\right)^2G(\alpha)+2\right] \tag{D22}$$

or, in a nondimensional form,

$$Z\left(\frac{a}{b}\right)=\left(\frac{\alpha}{1-\alpha}\right)^2G(\alpha)+2. \tag{D23}$$

From this

$$\frac{dZ}{d\alpha}=\left(\frac{\alpha}{1-\alpha}\right)^2\left(\frac{2G(\alpha)}{\alpha(1-\alpha)}+\frac{dG(\alpha)}{d\alpha}\right),\qquad \frac{dG}{d\alpha}=-19.69+74.28\alpha-107.52\alpha^2+52.48\alpha^3. \tag{D24}$$

References

[1] A. Hillerborg, M. Modéer and P.E. Petersson, "Analysis of Crack Formation and Crack Growth in Concrete by Means of Fracture Mechanics and Finite Elements", Cement and Concrete Research, Vol. 6, 1976, pp. 773–782.

[2] P.E.- Petersson, "Fracture Energy of Concrete: Method of Determination", Cement and Concrete Research, Vol. 10, 1980, pp. 78–89, and "Fracture Energy of Concrete: Practical Performance and Experimental Results", Cement and Concrete Research, Vol. 10, pp. 91–101.

[3] J.M. Krafft, A.M. Sullivan, R.W. Boyle, "Effect of Dimensions on Fast Fracture Instability of Notched Sheets", Cranfield Symposium, 1961, Vol. I, pp. 8–28.

[4] J.R. Rice, *The Mechanics of Quasi-Static Crack Growth*, Technical Report No. 63, prepared for Dept. of Energy, Brown University, Providence, R.I., October 1978.

[5] P.E. Petersson, *Crack Growth and Development of Fracture Zones in Plain Concrete and Similar Materials, Division of Building Materials*, Lund Institute of Technology, Sweden, Rep. TVBM-1006, Lund, October 1981.

[6] R.G. Hoagland, G.T. Hahn and A.R. Rosenfield, *Rock Mechanics*, Vol. 5 (1973), pp. 77–106.

[7] R.A. Schmidt and T.J. Lutz, "K_{IC} and J_{IC} of Westerly Granite–Effects of Thickness and In-plane Dimensions", 11th National Symposium on Fracture Mechanics, 1978.

[8] M.P. Wnuk and T. Mura, "Stability of a Disc-Shaped Geothermal Reservoir Subjected to Hydraulic and Thermal Loadings", Int. J. Fract. Mechanics, Vol. 17 (1981), pp. 493–517.

[9] B. Cotterell, "Plane Stress Ductile Fracture", in *Proceedings of International Conference on Fracture Mechanics and Technology*, University of Hong Kong, Vol. 2, pp. 785–795, edited by G.C. Sih and C.L. Chow, Sijthoff and Noordhoff, Int. Publishers, The Netherlands, 1977.

[10] K.B. Broberg, "On the Treatment of the Fracture Problem at Large Scale Yielding", ibid, pp. 837–858.

[11] K.J. Miller and A.P. Kfouri, "A Comparison of Elastic-Plastic Fracture Parameters in Biaxial Stress States", paper presented at 10th Natl. Symposium on Fracture Mechanics, published in ASTM STP 668.

[12] A.P. Kfouri and J.R. Rice, "Elastic/Plastic Separation Energy Rate for Crack Advance in Finite Growth Steps", in *Proceedings of ICF4, Advances in Research on the Strength and Fracture of Materials*, Vol. 1, p. 41, edited by D.M.R. Taplin, Pergamon Press, New York.

[13] J.R. Rice, "Mathematical Analysis in the Mechanics of Fracture", in *Fracture: An Advanced Treatise*, edited by H. Liebowitz, Vol. II, Mathematical Fundamentals, Ch. 3, pp. 191–311, Academic Press, New York.

[14] A. Hillerborg, M.S. Modéer and P.E. Petersson, "Analysis of Crack Formation and Crack Growth in Concrete by Means of Fracture Mechanics and Finite Elements", Cement and Concrete Research, Vol. 6, 1976, pp. 773–782.

[15] P.F. Walsch, "Fracture of Plain Concrete", The Indian Concrete Journal, Vol. 46, No. 11, November 1979, pp. 469, 470, and 476.

[16] J.H. Brown, "Measuring the Fracture Toughness of Cement Paste and Mortar", Magazine of Concrete Research, Vol. 24, No. 81, December, 1972, pp. 185–196.

[17] V.M. Entov and V.I. Yagust, "Experimental Investigation of Laws Governing Quasi-Static Development of Macrocracks in Concrete", Mechanics of Solids (translation from Russian), Vol. 10, No. 4, 1975, pp. 87–95.

[18] O.E. Gjorv, S.I. Sorensen and A. Arnesen, "Notch Sensitivity and Fracture Toughness of Concrete", Cement and Concrete Research, Vol. 7, 1977, pp. 333–344.

[19] C.M.J. Huang, "Finite Element and Experimental Studies of Stress Intensity Factors for Concrete Beams", Thesis Submitted in Partial Fulfillment of the Requirements for the Degree of Doctor of Philosophy, Kansas State University, Kansas, 1981.

[20] M.F. Kaplan, "Crack Propagation and the Fracture of Concrete", American Concrete Institute Journal, Vol. 58, No. 11, November 1961.

[21] C.E. Kesler, D.J. Naus and J.L. Lott, "Fracture Mechanics—Its Applicability to Concrete", International Conference on the Mechanical Behavior of Materials, Kyoto, August 1971.

[22] S. Mindess, F.V. Lawrence and C.E. Kesler, "The *J*-Integral as a Fracture Criterion for Fiber Reinforced Concrete", Cement and Concrete Research, Vol. 7, 1977, pp. 731–742.

[23] D.J. Naus, "Applicability of Linear-Elastic Fracture Mechanics to Portland Cement Concretes", Thesis Submitted in Partial Fulfillment of the Requirements for the Degree of Doctor of Philosophy, University of Illinois at Urbana-Champaign, 1971.

[24] S.P. Shah and F.J. McGarry, "Griffith Fracture Criterion and Concrete", Journal of the Engineering Mechanics Division, ASCE, Vol. 97, No. EM6, Proc. Paper 8597, December, 1971, pp. 1663–1676.

[25] C. Sok, J. Baron and D. François, "Mécanique de la Rupture Appliquée au Béton Hydraulique", Cement and Concrete Research, Vol. 9, 1979, pp. 641–648.

[26] S.E. Swartz, K.K. Hu, M. Fartash and C.-M.J. Huang, "Stress Intensity Factors for Plain Concrete in Bending—Prenotched Versus Precracked Beams", Report, Department of Civil Engineering, Kansas State University, Kansas, 1981.

[27] M. Wecharatana and S.P. Shah, "Resistance to Crack Growth in Portland Cement Composites", Report, Department of Material Engineering, University of Illinois at Chicago Circle, Chicago, Illinois, Nov. 1980.

[28] Z.P. Bažant and B.H. Oh, *Concrete Fracture Via Stress-Strain Relations*, Report No. 81-10/665c, Center for Concrete and Geomaterials, Northwestern University, Evanston, Oct. 1981.

[29] Z.P. Bažant and B.H Oh, "Crack Band Theory for Fracture of Concrete", Materials and Structures (RILEM, Paris), Vol. 16, 1983, pp. 155–177.

[30] J.R. Rice and E.P. Sorenson, "Continuing Crack Tip Deformation and Fracture for Plane-Strain Crack Growth in Elastic-Plastic Solids", J. Mech. Physics of Solids, Vol. 26, pp. 163–186.

[31] J.R. Rice, W.J. Drugan and T.C. Sham, *Elastic Plastic Analysis of Growing Cracks*, Tech. Rep. No. 65, Brown University, Providence, RI.

[32] W.G. Knauss, "On the Steady Propagation of a Crack in a Viscoelastic Sheet: Experiments and Analysis", Symposium on Fracture at Battelle Memorial Institute, in *The Deformation in Fracture of High Polymers*, ed. by H.H. Kausch, Publ. Plenum Press, 1971, pp. 501–541.

[33] M.P. Wnuk, "Accelerating Crack in a Viscoelastic Solid Subject to Subcritical Stress Intensity", in *Proceedings of Int. Conf. on Dynamic Crack Propagation*, Lehigh University, pp. 273–280, ed. G.C. Sih.

[34] M.P. Wnuk and T. Mura, "Effect of Microstructure on the Upper and Lower Limits of material Toughness in Elastic-Plastic Fracture", J. Mat. Sci., Vol. 4.

[35] D. Brock, *Elementary Engineering Fracture Mechanics*, Noordhoff International Publishing, Leyden, Netherlands, 1974.

[36] Z.P. Bažant and L. Cedolin, "Approximate Linear Analysis of Concrete Fracture by R-Curves", J. of Structural Engineering ASCE, Vol. 110, 1984, pp. 1336–1355.

[37] Z.P. Bažant *Mechanics of Fracture and Progressive Cracking in Concrete Structures*, Report 82-3/428m, Center for Concrete and Geomaterials, Northwestern University, Evanston, Illinois, to appear as a chapter in *Applications of Fracture Mechanics to Concrete Structures*, ed. by G. Sih, Martinus Nijhoff, 1984.

[38] I.N. Sneddon and M. Lowengrub, "Crack Problems in the Classical Theory of Elasticity", *The SIAM Series in Applied Mathematics*, John Wiley and Sons, Inc., New York.

[39] H. Tada, P. Paris and G. Irwin, *The Stress Analysis of Cracks Handbook*, Del Research Corporation, Hellertown, Pennsylvania, 1973.